UNIFORMED SERVICES UNIVERSITY OF THE HEALTH SCIENCES
F. EDWARD HÉBERT SCHOOL OF MEDICINE
4301 JONES BRIDGE ROAD
BETHESDA, MARYLAND 20814-4799

March 8, 2006

APPROVAL SHEET

Title of Dissertation: "Molecular mechanisms of Bcll0-mediated NF-κB signal transduction"

Name of Candidate: Felicia Langel
Doctor of Philosophy Degree
4 April 2004

Dissertation and Abstract Approved:

Chou-Zen Giam, Ph.D.   4-8-06
Department of Microbiology & Immunology   Date
Chairperson

Brian Schaefer, Ph.D.   4/4/06
Department of Microbiology & Immunology   Date
Major Advisor
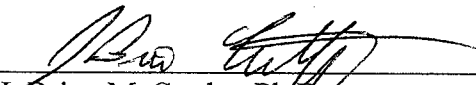
Charles Via, Ph.D.   4/4/06
Department of Pathology   Date
Member
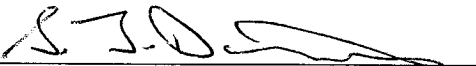
J. Brian McCarthy, Ph.D.   4/4/06
Department of Pharmacology   Date
Member

Stephen Davies, Ph.D.   4/4/06
Department of Microbiology & Immunology   Date
Member
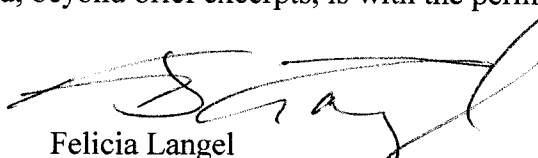
Report Documentation Page		*Form Approved* *OMB No. 0704-0188*

Public reporting burden for the collection of information is estimated to average 1 hour per response, including the time for reviewing instructions, searching existing data sources, gathering and maintaining the data needed, and completing and reviewing the collection of information. Send comments regarding this burden estimate or any other aspect of this collection of information, including suggestions for reducing this burden, to Washington Headquarters Services, Directorate for Information Operations and Reports, 1215 Jefferson Davis Highway, Suite 1204, Arlington VA 22202-4302. Respondents should be aware that notwithstanding any other provision of law, no person shall be subject to a penalty for failing to comply with a collection of information if it does not display a currently valid OMB control number.

1. REPORT DATE **MAR 2006**	2. REPORT TYPE	3. DATES COVERED **00-00-2006 to 00-00-2006**
4. TITLE AND SUBTITLE **Molecular Mechanisms of Bcl10-Mediated NF-kappaB Signal Transduction**		5a. CONTRACT NUMBER
		5b. GRANT NUMBER
		5c. PROGRAM ELEMENT NUMBER
6. AUTHOR(S)		5d. PROJECT NUMBER
		5e. TASK NUMBER
		5f. WORK UNIT NUMBER
7. PERFORMING ORGANIZATION NAME(S) AND ADDRESS(ES) **Uniformed Services University of the Health Sciences,F. Edward Hebert School of Medicine,4301 Jones Bridge Road,Bethesda,MD,20814-4799**		8. PERFORMING ORGANIZATION REPORT NUMBER
9. SPONSORING/MONITORING AGENCY NAME(S) AND ADDRESS(ES)		10. SPONSOR/MONITOR'S ACRONYM(S)
		11. SPONSOR/MONITOR'S REPORT NUMBER(S)

12. DISTRIBUTION/AVAILABILITY STATEMENT
Approved for public release; distribution unlimited

13. SUPPLEMENTARY NOTES

14. ABSTRACT

Bcl10 is a key signaling intermediate in the TCR-to-NF-κB pathway in T lymphocytes. It is currently believed that, once activated, Bcl10 functions within a multiprotein signaling complex that activates the IKK complex. Bcl10 is thought to regulate this signaling complex, but how it transmits its signal through the complex is unknown. A thorough knowledge of Bcl10 biology is critical to understanding how Bcl10 functions and how it regulates its binding partners. In this study, we used mutational analysis molecular imaging, biochemistry, and computer/bioinformatics modeling to elucidate a structure and function for Bcl10. From our data, we identified a novel binding site for MALT1 within the Bcl10 protein, hypothesized that this site is completely separate and distinct from the binding sites of other Bcl10 signaling partners, and proposed two regulatory functions for the Bcl10 C-terminus. These findings suggest that Bcl10 has multiple functional domains and, hence, that Bcl10 molecular biology is more complex than previously thought. These observations serve to emphasize Bcl10's role as a crucial regulator of the TCR-to-NF-κB signaling pathway.

15. SUBJECT TERMS

16. SECURITY CLASSIFICATION OF:			17. LIMITATION OF ABSTRACT	18. NUMBER OF PAGES	19a. NAME OF RESPONSIBLE PERSON
a. REPORT **unclassified**	b. ABSTRACT **unclassified**	c. THIS PAGE **unclassified**	**Same as Report (SAR)**	**100**	

Standard Form 298 (Rev. 8-98)
Prescribed by ANSI Std Z39-18

The author hereby certifies that the use of any copyrighted material in the thesis manuscript entitled:

"Molecular mechanisms of Bcl10-mediated NF-κB signal transduction"

is appropriately acknowledged and, beyond brief excerpts, is with the permission of the copyright owner.

Felicia Langel
Molecular and Cell Biology Program
Uniformed Services University

Abstract

Title: Molecular Mechanisms of Bcl10-Mediated NF-kappaB Signal Transduction

Author: Felicia D. Langel, Ph.D., 2006

Directed by: Brian C. Schaefer, Ph.D., Assistant Professor, Department of Microbiology and Immunology

Bcl10 is a key signaling intermediate in the TCR-to-NF-κB pathway in T lymphocytes. It is currently believed that, once activated, Bcl10 functions within a multi-protein signaling complex that activates the IKK complex. Bcl10 is thought to regulate this signaling complex, but how it transmits its signal through the complex is unknown. A thorough knowledge of Bcl10 biology is critical to understanding how Bcl10 functions and how it regulates its binding partners. In this study, we used mutational analysis, molecular imaging, biochemistry, and computer/bioinformatics modeling to elucidate a structure and function for Bcl10. From our data, we identified a novel binding site for MALT1 within the Bcl10 protein, hypothesized that this site is completely separate and distinct from the binding sites of other Bcl10 signaling partners, and proposed two regulatory functions for the Bcl10 C-terminus. These findings suggest that Bcl10 has multiple functional domains and, hence, that Bcl10 molecular biology is more complex than previously thought. These observations serve to emphasize Bcl10's role as a crucial regulator of the TCR-to-NF-κB signaling pathway.

MOLECULAR MECHANISMS OF Bcl10-MEDIATED

NF-kappaB SIGNAL TRANSDUCTION

by

Felicia D. Langel

Dissertation submitted to the

Faculty of the Molecular and Cell Biology Program

Uniformed Services University of the Health Sciences

in partial fulfillment of the requirements for the degree of

Doctor of Philosophy 2006

Table of Contents

Table of Figures

Table of Tables

Glossary

AP-1 (activator protein 1): a transcription factor consisting of a homo- or heterodimeric complex comprising members of the jun, fos, ATF, and Maf protein families

APC (antigen presenting cell): a cell that displays foreign antigen complexed with MHC on its surface

API2 (apoptosis inhibitor-2): a member of the inhibitor of apoptosis protein gene family implicated in MALT B cell lymphoma

Bcl10 (B cell lymphoma 10): a key adaptor protein in the NF-κB signaling pathway

BCR (B cell receptor): cell-surface receptor of B cells that binds to cognate antigen

β-galactosidase: the product of the LacZ gene that metabolizes lactose into glucose and galactose

BinCARD (Bcl10-interacting protein with CARD): a CARD protein capable of inhibiting Bcl10-mediated activation of NF-κB, via CARD-CARD interaction with Bcl10

CARD (caspase recruitment domain): three-dimensional protein domain involved in protein-protein interactions and found in many molecular mediators of apoptosis

CARMA1 (CARD-containing MAGUK protein 1): scaffolding protein involved in the NF-κB signaling pathway

CC domain (coiled-coil domain): a protein structural motif consisting of 2-5 alpha-helices coiled together that often mediates protein-protein interactions

CD3: a critical signaling component of the T cell receptor complex

CD4: a co-receptor for the T cell receptor expressed on the surface of T helper cells

CD8: a co-receptor for the T cell receptor expressed on the surface of cytotoxic T cells

CD25: the α chain of the high-affinity interleukin-2 receptor

CD28: T cell-surface antigen that provides co-stimulatory signals required for naïve T cell activation

cDNA (complementary DNA): DNA synthesized from an RNA template

CH12 B cell: a B cell line with an H-2^k MHC haplotype that is derived from a murine B cell lymphoma

D10-IL2 T cell: a murine CD4$^+$ T cell clone dependent upon exogenous IL-2 supplementation for its growth and survival, and which is responsive to a conalbumin peptide presented by I-A^k

DD (death domain): a protein-protein interaction domain present in several proteins involved in apoptosis and NF-κB signaling

EST (expressed sequence tag): a cDNA-derived portion of an open reading frame that can be used to identify the full gene

FACS (fluorescence-activated cell sorting): methodology that uses lasers and microfluidic cell separation to identify unique cell types based upon differences in cell fluorescence

FLAG-tag: a polypeptide tag added to a recombinant expressed protein, used for detection with specific anti-FLAG antibodies

GFP (green fluorescent protein): a variant of the gene first isolated from the jellyfish, *A. victoria*; the expressed fluorescent protein is used as a genetic marker

GUK domain (guanylate kinase domain): a guanylate kinase-like domain lacking catalytic activity and facilitating protein-protein interactions

3xHA-tag (triple hemagglutinin tag): influenza virus hemagglutin tag added to a recombinant expressed protein, used for detection with specific anti-HA antibodies

HEK-293T cell: an SV40-transformed cell line derived from human embryonic kidney cells

ICAM-1 (intercellular adhesion molecule 1): molecule displayed on the surface of an antigen presenting cell capable of binding LFA-1 on the surface of a T cell

Ig-like (immunoglobulin-like): a glycoprotein domain structurally resembling the canonical immunoglobulin domain, originally identified by structural analysis of the antibody molecule

IκB (inhibitor of κB): an inhibitor protein that binds to the NF-κB dimer and holds it in its inactive state in the cytoplasm

IKK complex (IκB kinase complex): a trimeric protein complex comprising a regulatory subunit (IKKγ) and two serine/threonine kinases (IKKα and IKKβ) involved in the activation of NF-κB, via phosphorylation of the IκB target

IL-1R (interleukin-1 receptor): a cell-surface receptor that binds interleukin-1, a cytokine secreted by macrophages and many other cell types

IL-2 (interleukin-2): an autocrine cytokine secreted by T cells that stimulates T cell growth and differentiation

IS (immunological synapse): antigen-dependent site of transient intercellular contact between immune cells resulting in protein segregation into membrane domains

ITAM (immunoreceptor tyrosine-based activation motif): phosphorylated tyrosines in this motif recruit positive signaling effector molecules to transmembrane receptors, such as the TCR/CD3 complex

LFA-1 (lymphocyte functional antigen 1): a leukocyte cell adhesion integrin molecule, which binds to ICAM-1

LPS (lipopolysaccharide): integral part of the outer cell membrane of gram-negative bacteria

MAGUK (membrane-associated guanylate kinase): a superfamily of proteins that serve as scaffolds to build multi-protein complexes at the plasma membrane

MALT (mucosa-associated lymphoid tissue): acronym used to refer to lymphoid tissue of the mucosa; also a type of B cell lymphoma and a signaling intermediate in the NF-κB pathway (MALT1), which is a chromosomal translocation target in MALT lymphoma

MHC (major histocompatibility complex): genomic region that encodes for cell-surface molecules that present peptide antigen to the T cell receptor

MIRR (multichain immune recognition receptor): immune cell-surface receptor that associates with Src-family kinases to initiate signaling

MMLV (Moloney murine leukemia virus): enveloped retrovirus capable of integrating into the host genome

MSCV (murine stem cell virus): a variant of MMLV, which allows reliable expression in immune cells

MZL (marginal zone lymphoma): lymphoma of a type of B cell arising from the region between the non-lymphoid red pulp and the lymphoid white pulp of the spleen; this subset includes MALT lymphoma

NFAT (nuclear factor of activated T cells): a calcineurin-dependent transcription factor involved in the regulation of interleukin-2 and interleukin-4 gene transcription

NF-κB (nuclear factor of kappa light chain gene enhancer in B cells): a transcription factor consisting of a homo- or heterodimeric complex involved in the regulation of inflammatory and immune responses

PAMPs (pathogen-associated molecular patterns): small molecular sequences consistently associated with pathogens, frequently recognized by receptors of the innate immune system

pBlueScript: cloning vector containing several features including multiple cloning sites, Amp^R, and LacZ

pcDNA: vector designed for high-level stable and transient expression in mammalian cells, containing a CMV promoter, multiple cloning sites, and a Neo^R gene

pCL-Eco: retrovirus packaging vector containing the GAG, POL, and ENV genes of MMLV

PDK1 (3-phosphoinositide-dependent kinase 1): serine/threonine protein kinase whose activity depends upon phosphatidylinositol 3-kinase (PI3K)

PDZ domain: named for the first three proteins in which this conserved sequence was first recognized; this domain mediates protein-protein interactions

pENeo: replication defective MMLV retrovirus containing an IRES- Neo^R cassette

PKCθ (protein kinase C θ): a protein kinase isozyme that phosphorylates specific serines and threonines on a variety of intracellular signaling proteins; tissue-restricted expression to T cells, skeletal muscle, and a few other cells/tissues

PLCγ1 (phospholipase C γ1): a key enzyme in phosphatidylinositol (PIP$_2$) metabolism

POLKADOTS (punctuate and oligomeric killing or activating domains transducing signals): oligomers of Bcl10 and MALT1 resembling cytoplasmic structures that recruit caspases and trigger apoptosis

RIP2 (receptor interacting serine-threonine kinase 2): an NF-κB-activating and cell death-inducing kinase

SDS-PAGE (sodium dodecyl sulfate-polyacrylamide gel electrophoresis): a common technique for separating denatured proteins by size

SH3 (Src homology 3): conserved amino acid domain, consisting to two anti-parallel β sheets, that mediates interactions between proteins

SMAC (supramolecular activation cluster): region of the immunological synapse consisting of either a central (c) or peripheral (p) protein segregation membrane domain

TCR (T cell receptor): cell-surface receptor of T cells that binds a peptide of processed cognate antigen complexed with MHC

TLR (Toll-like receptor): transmembrane receptor that recognizes PAMPs and activates immune cells of the innate immune system

TNFR (tumor necrosis factor receptor): a cell-surface receptor that binds tumor necrosis factor, a cytokine secreted by macrophages and other cell types

TRAF6 (TNF receptor-associated factor 6): ubiquitin ligase that serves as a catalytic intermediate in several signaling cascades, particularly those terminating with the activation of NF-κB

Chapter 1. Introduction

In the adaptive immune response, T lymphocytes (helper and cytotoxic) become

activated through interactions with antigen presenting cells (APCs). APCs, specifically

dendritic cells, macrophages, and B cells, carry foreign peptide antigen bound to MHC

class I and II molecules displayed on their cell surfaces (10). T cells recognize these

antigen-MHC complexes through the T cell receptor (TCR), a member of the multichain

immune recognition receptor (MIRR) family (12). The TCR is comprised of i) the

transmembrane α and β chains, which are the components that specifically recognize

MHC-bound peptide ligand, ii) the associated transmembrane ε, γ, and δ chains (termed

CD3), and iii) the ζ chain. The CD4 and CD8 co-receptors stabilize the association

between the TCR and its ligand by binding cooperatively with the TCR to the MHC class

I and class II molecules, respectively (52). Immediately following TCR ligation, T cell

activation commences with the rapid recruitment and activation of upstream signaling

molecules. The first such molecules to arrive at the site of TCR activation are the Src

kinases, Lck and Fyn which tyrosine phosphorylate immunoreceptor tyrosine-based

activation motifs (ITAMs) on the intracellular domains of CD3ε, γ, δ, and TCRζ (91).

This results in the recruitment and activation of the kinase, ZAP-70 which, upon binding

to the phosphorylated ITAMs, tyrosine phosphorylates several recruited adaptor

molecules, including SLP-76, LAT, Grb2, and Vav1 (1). This early tyrosine

phosphorylation cascade leads to the initiation of several downstream signaling cascades

that are essential for sustained T cell activation and, ultimately, for T cell differentiation

and survival (*Figure 1*).
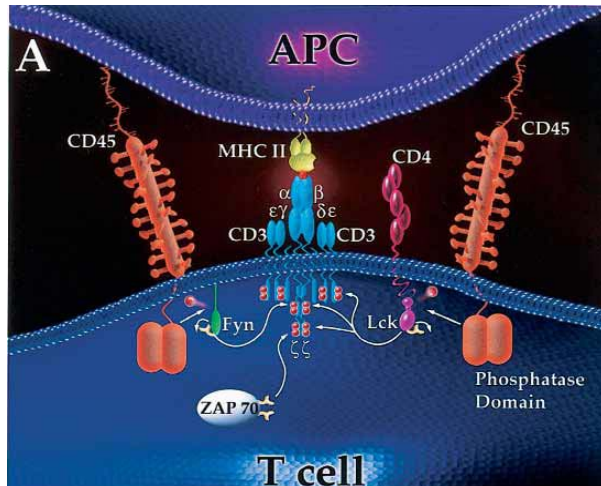
Figure 1. TCR-induced early tyrosine phosphorylation cascade
     Immediately following TCR binding of antigen/MHC, the Src-kinases, Lck and Fyn, are activated and phosphorylate ITAMs on the intracellular domains of CD3ϵ, γ, δ, and TCRζ. This results in the recruitment and activation of ZAP-70.
(Nel 2002. *J Allergy Clin Immunol 109:758*)

Assembly of the IS is necessary for sustained T cell signaling

The recruitment of signaling molecules to the TCR is not haphazard, as these molecules soon form a molecular arrangement known as the immunological synapse (IS). Utilizing fluorescently-labeled antibodies to identify signaling molecules known to associate with the TCR, Monks, et al. demonstrated that, over several hours, signaling and adaptor molecules spatially segregate at the site of TCR activation (49). Further investigation of these spatially segregated supramolecular activation clusters (SMACs) led investigators to define a central (cSMAC) zone and a peripheral (p-SMAC) zone, resembling a bull's-eye configuration (13, 49). The p-SMAC is characterized by a ring of LFA-1 bound to its APC ligand, ICAM-1. It is believed that this interaction helps to stabilize the IS (23, 49). In support of this hypothesis, reorganization of the actin cytoskeleton accompanies formation of the IS, whereby the cytoplasmic tail of LFA-1 is believed to bind directly to the cytoskeleton (38, 54, 65). The c-SMAC contains the cytoplasmic molecules involved in T cell signaling, as well as the transmembrane co-stimulatory molecule CD28 which is critical for naïve T cell activation (23, 34). The functional role of the c-SMAC is controversial and several models have been proposed.

Among these are that the c-SMAC may represent a polarized surface for which

biochemical interactions between signaling molecules can occur (50), or it may serve as

an enhancement to signaling by excluding and including particular enzymatic substrates

(21). Evidence supporting the latter model comes from the observation that several

signaling intermediates stably enter lipid rafts (membrane lipid microdomains) at the site

of the IS following TCR activation (87). Alternatively, some evidence suggests that the

c-SMAC ultimately serves to attenuate T cell activation by triggering TCR degradation

(26, 41). Finally, one report has suggested that sustained T cell activation can occur prior

to the maturation of the IS, suggesting that the IS forms subsequent to very early T cell

signaling events (42) (*Figure 2*).
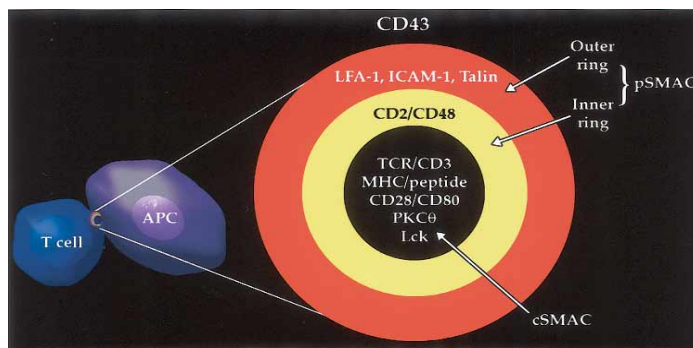
Figure 2. The mature immunological synapse
Cross-section of the IS showing the arrangement of receptors, signaling molecules, and cytoskeletal proteins in the p-SMAC and c-SMAC. (Nel 2002. *J Allergy Clin Immunol 109:758*)

T cell activation initiates several signaling pathways

Immediately downstream of early tyrosine phosphorylation events, are several

signaling cascades that lead to gene transcription. In one such cascade, phospholipase C

γ1 (PLCγ1) is recruited to the immunological synapse where it is phosphorylated.

Phosphorylation activates the PLCγ1 enzyme, which cleaves phosphatidylinositol-4,5

biphosphate (PIP_2) to generate inositol-1,4,5-trisphosphate (IP_3). IP_3 releases Ca^{2+} from

intracellular calcium stores in the endoplasmic reticulum, and this signal directly triggers

an extracellular Ca^{2+} influx (4). T cell calcium flux activates calcineurin, which

dephosphorylates the transcription factor, nuclear factor of activated T cells (NFAT), and allows it to enter the nucleus where it activates the interleukin-2 (IL-2) promoter (54). IL-2 is an autocrine growth factor of T cells. In another such signaling pathway, the diacylglycerol-regulated protein, Ras-GRP activates the GTPase, Ras (p21ras). Ras activation leads to activation of the ERK pathway, resulting in the expression of c-Fos, a component of the heterodimer activator protein 1 (AP-1) transcription factor, involved in the regulation of the IL-2 promoter (31). Another pathway involves CD28 co-stimulation dependent activation of JNK1 leading to the phosphorylation of c-Jun, another component of AP-1, which is also involved in IL-2 transcription (76). Additionally, a pathway involving PI-3 kinase activation serves to anchor PLCγ1 and Vav1 to the membrane, thereby recruiting and activating the kinase, Akt, which is a critical mediator of pro-survival signals (3) (*Figure 3*).
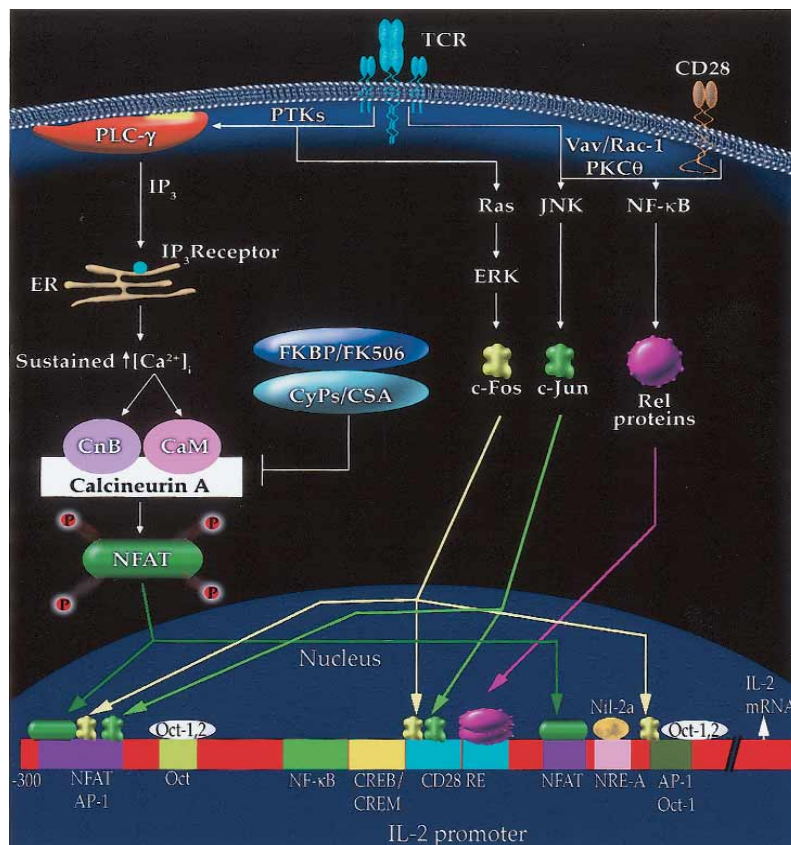
Figure 3. TCR-induced signaling pathways
Schematic of the multiple pathways leading to the activation of the IL-2 promoter. Ca^{2+}/calcineurin, Ras/MAP (JNK), and NF-κB signaling cascades are represented.
 (Nel 2002. *J Allergy Clin Immunol 109:758*)

The NF-κB pathway is crucial to the adaptive immune response

Perhaps the most critical TCR-induced signaling cascade is the one leading to nuclear factor (NF)-κB activation. NF-κB, and the aforementioned NFAT and AP-1, are all required for optimal IL-2 production and cooperatively regulate the transition of a naïve resting T cell to an activated effector T cell. However, NF-κB activation also triggers many other essential T cell functions, and activation of this transcription factor is thus critical for adaptive immune function. Murine knockout studies of several key upstream intermediates of the NF-κB pathway (to be discussed in more detail later in this chapter) have demonstrated that a defect in the NF-κB pathway leads to a profound defect in T cell proliferation and differentiation. More precisely, defects in the NF-κB pathway prevent T cells from entering S phase of the cell cycle upon TCR stimulation (60). Once activated, resting T cells enter S phase, at least in part, as a consequence of upregulation of IL-2 and the IL-2 receptor α chain (CD25) (72). A defect in the NF-κB pathway prevents the upregulation of IL-2 and CD25, with the cumulative effect being to prevent the T cell from proliferating, differentiating, and gaining effector functions required for a normal adaptive response (60, 61, 80, 89).

It is important to note that the NF-κB signaling pathway is not only involved in T cell activation. In contrast, it is a ubiquitous signal transduction pathway found in a variety of cell types. The signaling cascade begins at the cell surface when ligands bind to specific cell-surface receptors. The cascade culminates with the activation of NF-κB in the cell cytoplasm and its subsequent translocation to the nucleus (45). The NF-κB family of transcription factors, including p65 (RelA) and p50, typically form heterodimers upon activation and activate genes for promoters encoding cytokines,

chemokines, stress-response proteins, and anti-apoptotic proteins (22, 45). The canonical

pathway to NF-κB activation proceeds through the trimeric IκB kinase (IKK) complex.

The IKK complex is composed of two catalytic subunits (IKKα and IKKβ) and a

regulatory subunit (IKKγ/NEMO) (45). Activation of the IKK complex allows IKKβ to

phosphorylate inhibitor of (I) κB. IκB, in its unphosphorylated form, binds to and

sequesters the NF-κB heterodimer (p65/p50) in the cell cytoplasm. Phosphorylation of

IκB targets it for ubiquitination and subsequent degradation by the 26S proteasome (36),

thereby freeing NF-κB to translocate to the nucleus and bind target DNA (62) (*Figure 4*).
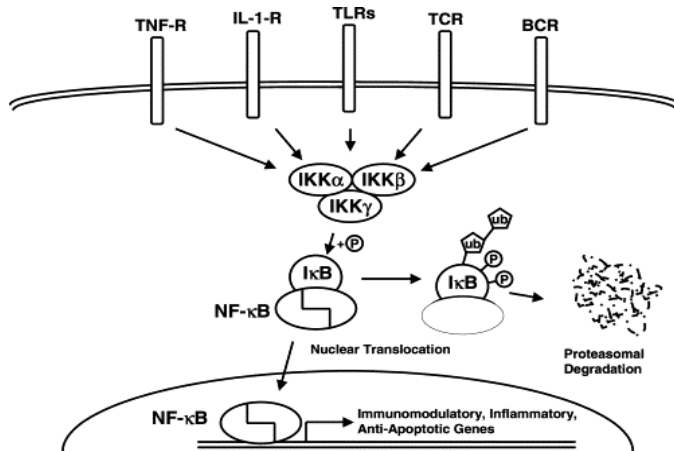
Figure 4. The classical NF-κB pathway
    NF-κB activation is triggered by the ligation of many distinct cell-surface receptors. The pathways converge at the IKK complex, where the activation of the complex results in IKKβ phosphorylation of IκB. This leads to the ubiquitination of IκB and its degradation by the proteasome, thereby allowing NF-κB to translocate to the nucleus.
(Ruland et al. 2003. *Sem Immunol 15:177*)

The NF-κB pathway in lymphocytes is initiated by PAMPs, cytokines, and antigen

In the innate and adaptive immune responses, NF-κB activation is triggered by the

stimulation of specific cell-surface receptors. These receptors [Toll-like receptors

(TLRs), interleukin-1 receptor (IL-1R), tumor necrosis factor receptor (TNFR), B cell

receptor (BCR), and TCR] activate distinct signaling pathways that converge at the level

of the IKK complex (62). The cells of the innate immune system (e.g., macrophage,

neutrophil, dendritic cell, and natural killer cell) display TLRs on their surfaces that

recognize pathogen-derived substances such as lipopolysaccharide (LPS), peptidoglycan,

lipoprotein, and double-stranded RNA (81). Such pathogen associated molecular patterns

(PAMPs) bind to TLRs, initiating a signaling cascade that recruits MyD88 and IRAK to

the plasma membrane. The ubiquitin ligase, TRAF6 is subsequently ubiquitinated and

activates the IKK complex (88). IL-1Rs and TNFRs are found on cells of both the innate

and adaptive immune systems and are triggered by binding various cytokines, such as IL-

1 and TNF. This pathway recruits TRADD and TRAF2 to the plasma membrane, leading

to the activation of the kinases, RIP and MEKK3, and ultimately resulting in the

activation of the IKK complex (45) (*Figure 5*).
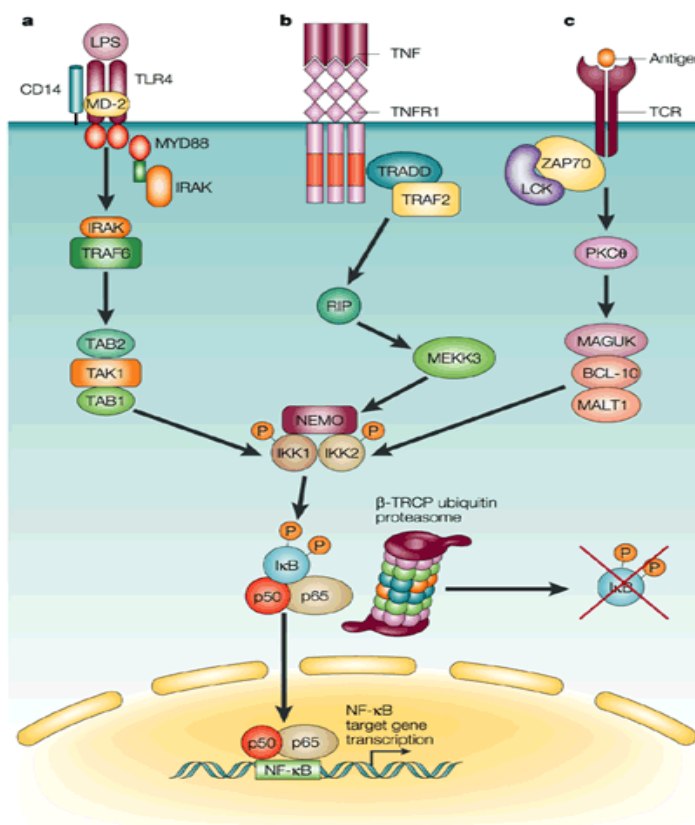
Figure 5. Multiple pathways to NF-κB activation
   Three examples of upstream signaling cascades leading to the activation of the IKK complex and subsequent NF-κB activation: **a.** LPS binding to TLR4 recruits MyD88 and IRAK. Activation of IRAK results in the ubiquitination of TRAF6 and possible signal transmission through the TAK1-TAB1-TAB2 complex to the IKK complex. **b.** TNF binding to TNFR1 leads to TRADD followed by TRAF2 recruitment. Signaling proceeds through RIP and MEKK3 to the IKK complex. **c.** TCR ligation by antigen/MHC results in an initial phosphorylation cascade that recruits PKCθ. This leads to the activation of the Bcl10-MALT1-CARMA1 (MAGUK) complex, resulting in IKK complex activation.
(Verma et al. 2002. *Nat Rev Immunol 2:725*)

Interestingly, an alternative pathway to NF-κB activation has been recently

identified in which NIK kinase activates IKKα, leading to the nuclear translocation of a

different NF-κB heterodimer, p52/RelB. This alternative pathway is triggered by the cell-surface ligation of two members of the TNFR family, BAFF-R and CD40 (55).

BCRs and TCRs are found on B cells and T cells, respectively, and share similar pathways that lead to IKK complex activation. Antigen-induced signaling through the BCR and TCR results in NF-κB activation critical to growth and differentiation in both cell types (62). While it has been generally accepted that CD28 co-stimulation contributes to NF-κB activation in T cells (85), recent studies suggest that CD28 may preferentially activate NF-κB through PI-3 kinase and Akt rather than through upstream intermediates initiated by TCR ligation (34, 70). This suggests that TCR stimulation and CD28 co-stimulation can be uncoupled with respect to NF-κB activation.

NF-κB cell signaling is linked to lymphoma

Interestingly, specific abnormalities in BCR signaling to NF-κB are linked to lymphoma of mucosal B cells. Mucosa-associated lymphoid tissue (MALT) B cell lymphoma was first described in 1983 by Isaacson and Wright (28) and, years later, Isaacson observed that the primary etiologic agent for gastric MALT lymphoma is chronic infection with *Helicobacter pylori* (29). One hypothesis is that T cell responses to *H. pylori* antigens stimulate neoplastic growth of B cells (27), although it is also possible that direct antigen stimulation of B cells is responsible for this pre-neoplastic proliferation (16). MALT lymphomas, also known as marginal zone lymphomas (MZL), have additionally been associated with chronic inflammatory conditions and autoimmune diseases, such as bronchial-associated lymphoid hyperplasia in the lung and Sjogren's disease in the salivary glands (17, 75). MALT lymphoma arises as a consequence of essentially two types of chromosomal translocations in mucosa-associated B cells of a

marginal zone phenotype. The t(11;18)(q21;q21) translocation is the most common chromosomal abnormality (44) and results in the fusion of the apoptosis inhibitor-2 (API2) gene on chromosome 11 and the MALT1 gene on chromosome 18 (2). The resulting API2-MALT1 fusion protein can self-oligomerize and has deregulated ubiquitin ligase activity, so as to bypass normal upstream NF-κB signaling and potently activate NF-κB (2, 46, 84, 98). The t(1;14)(p22;q32) translocation relocates the entire coding region of the Bcl10 gene from chromosome 1 to chromosome 14, placing it under the control of the immunoglobulin heavy chain enhancer (93). The consequence of this mutation is to upregulate Bcl10 expression (97), which may result in MALT1 oligomerization and enhanced or spontaneous NF-κB activation (16, 83). The net effect of constitutive NF-κB activation in MALT lymphoma cells may be to provide a survival advantage to these malignant cells and/or to promote their proliferation (97) (*Figure 6*).
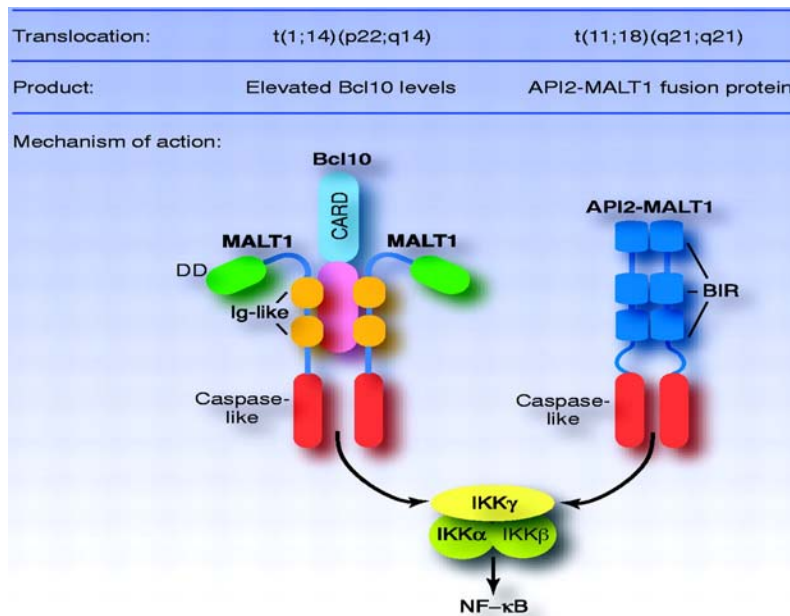
Figure 6. Chromosomal translocations in MALT B cell lymphoma
    The recurrent chromosomal translocation of t(1;14)(p22;q32) is believed to result in overexpression of Bcl10 leading to MALT1 oligomerization and excessive NF-κB activation. The t(11;18)(q21;q21) recurrent chromosomal translocation leads to the expression of the API2-MALT1 fusion protein that is thought to result in the potent activation of NF-κB (Lucas et al. 2004. *J Cell Sci 117:31*)

The antigen-dependent NF-κB pathway contains several unique signaling intermediates

PKCθ

Upon BCR and TCR ligation, and immediately following the early tyrosine phosphorylation cascade, a PLCγ1-induced Ca^{2+} flux activates protein kinase C (PKC) (30). PKC is an important second messenger in lymphocyte activation and it exists in several isoforms (α, $β_1$, $β_2$, γ, δ, ε, ν, θ, ζ, and λ) (7). Independent of the Ca^{2+} flux, the only PKC to be recruited to the IS upon TCR ligation is PKCθ (50). PKCθ is selectively expressed in T cells and platelets (48) and it also plays a role in JNK activation and AP-1 transcription, leading to IL-2 production (92). PKCθ's critical importance to T cell activation was established when it was reported that murine PKCθ^{-/-} T cells are unable to activate NF-κB following TCR stimulation. However, NF-κB activation as a consequence of TNFR ligation is unaffected in these cells, demonstrating the specific role of PKCθ in TCR signaling to NF-κB (80). It is unclear, however, how PKCθ is recruited to the IS and by what means it is activated, although it is known that the diacylglycerol-binding C1 domains of PKCθ are required for signal-induced membrane localization (8). A recent report suggests that 3-phosphoinositide-dependent kinase 1 (PDK1) functions upstream of PKCθ and may recruit it to lipid rafts of the IS where it is phosphorylated and activated (43). Previous evidence has suggested that PKCθ may also be recruited to the IS and IS-associated cytoskeleton by Vav1, a guanine nucleotide exchange factor (GEF) for Rac-1, which is involved in cytoskeleton assembly (18, 86).

Immediately downstream of PKCθ activation is a trimeric complex of proteins (B cell lymphoma 10 (Bcl10), mucosa-associated lymphoid tissue protein 1 (MALT1), and

CARD-containing MAGUK protein 1 (CARMA1)) that is equally critical to T cell

activation. Murine Bcl10$^{-/-}$, MALT1$^{-/-}$, or CARMA1$^{-/-}$ T cells are deficient in the TCR-

induced NF-κB pathway, leading to a failure of T cell activation, proliferation, and

differentiation (60, 61, 89). Bcl10, MALT1, and CARMA1 appear to behave similarly in

T and B cells. PKCβ serves as the homolog to PKCθ in B cells (64, 78) (*Figure 7*).
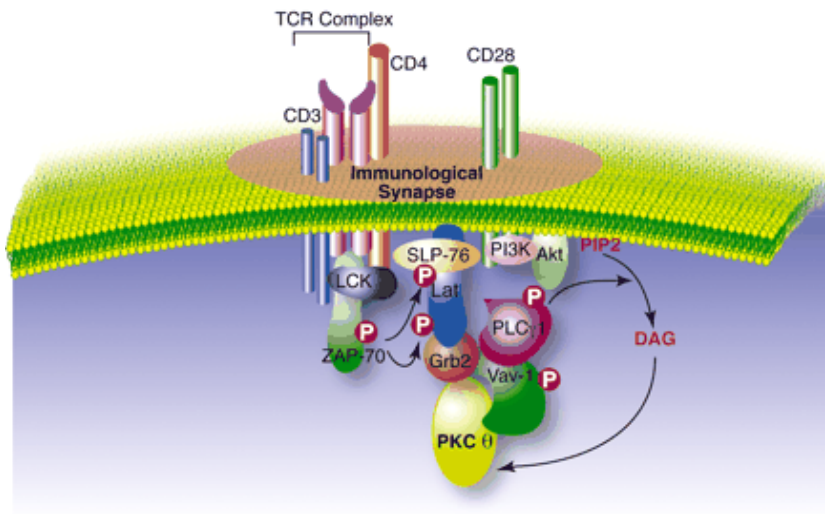
Figure 7. PKCθ is recruited to the IS
Upon T cell activation, several kinases and adaptor proteins are recruited to the IS. PKCθ is possibly recruited by PDK1 and/or by Vav1, however, the mechanism by which PKCθ is activated is unknown. (Lucas et al. 2004. *J Cell Sci 117:31*)

Bcl10

Bcl10 was independently identified as a signaling intermediate (it is an adaptor

protein) in the NF-κB pathway several times and, as such, was initially given several

names (CLAP, CIPER, cE10, and CARMEN). Bcl10 has been shown to be ubiquitously

expressed in tissues, positively regulates lymphocytes, activates NF-κB, and possesses an

N-terminus that is a homolog to the equine herpesvirus-2 protein E10 (39, 60, 73, 82).

Homology studies of Bcl10 reveal that it has an N-terminal caspase recruitment domain

(CARD), followed by a region capable of binding MALT1, and a C-terminus of unknown

homology that is rich in serines and threonines (46, 73, 82, 95) and is capable of being

phosphorylated (96). Deletion of the MALT1 binding site prevents MALT1 binding to

Bcl10 and abrogates NF-κB activation (46). Failure of RIP2, a CARD-containing

serine/threonine kinase, to phosphorylate Bcl10 correlates with defective TCR-induced

NF-κB activation (59). Bcl10 preferentially interacts with other CARD-containing

molecules through its CARD and has been shown to interact with CARD9, CARD10,

CARMA1 (CARD11), CARD14, RIP2, and BinCARD (5, 6, 20, 47, 56, 59, 94). Though

each of these interactions has been reported to trigger or inhibit NF-κB activation, not all

of these molecules have formally been shown to influence T cell proliferation and IL-2

production, and their physiological role in T cell activation is thus uncertain. Bcl10 is

capable of self-oligomerization (through its CARD) (39) and interacts directly with and

mediates the oligomerization and activation of MALT1 (46). Prior to T cell activation,

Bcl10 is predominantly cytoplasmic, but, upon TCR ligation, Bcl10 is recruited to lipid

rafts of the IS by CARMA1 (19). Bcl10 signaling may be downregulated by the

ubiquitin ligases, NEDD4 and Itchy, which target Bcl10 for degradation by the lysosomal

pathway (69). Additionally, the CARD-containing protein, BinCARD, has been shown

to interact with Bcl10, resulting in decreased amounts of phosphorylated Bcl10 and

potent suppression of NF-κB activation (94) (*Figure 8*).
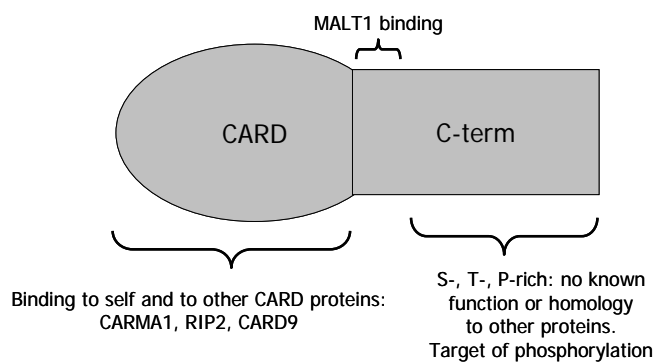
Figure 8. Schematic of Bcl10

MALT1

MALT1 (also called paracaspase) has been shown to be essential for T cell activation, required for normal development in B cells, and critical for antigen-dependent NF-κB activation in T and B cells (58, 61). MALT1 is expressed predominantly in peripheral blood mononuclear cells, but has been identified in multiple cell types at very low levels. MALT1 has an N-terminal death domain, followed by two immunoglobulin (Ig)-like domains, a region with homology to caspases (caspase-like domain), and a C-terminal region containing two TRAF6 binding domains. MALT1 interacts directly with Bcl10 upon T cell activation and facilitates binding to Bcl10 through its two Ig-like domains (46, 84). MALT1 activation is stimulated by and may require oligomerization, and its activity is also dependent upon the presence of its C-terminus, which includes the caspase-like domain and the TRAF6 binding sites (46, 79, 84). Following TCR activation, MALT1 is recruited to lipid rafts in the IS in a CARMA1-dependent manner and its caspase-like domain may interact directly with CARMA1 (9) (*Figure 9*).
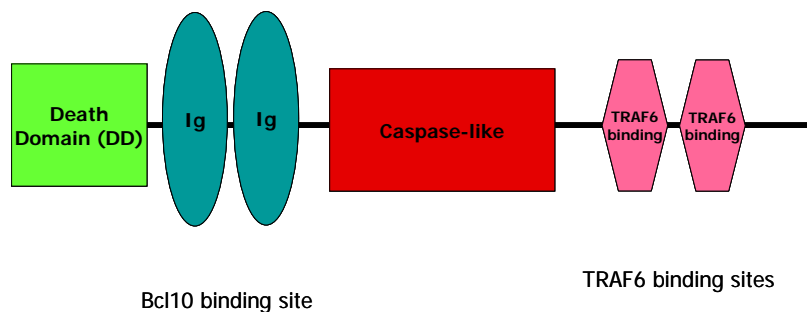
Figure 9. Schematic of MALT1

CARMA1

CARMA1 (also known as CARD11 and Bimp3) is predominantly expressed in lymphocytes (53), is necessary for antigen-dependent NF-κB activation in lymphocytes, is required for normal development in B cells, and induces proliferation and IL-2

production in T cells (14, 20, 53, 56, 89). CARMA1 is the only lymphocyte-specific

member of the membrane-associated guanylate kinase (MAGUK) family of scaffolding

proteins (14). MAGUK proteins are characterized by multiple protein-binding domains

(SH3, PDZ, and GUK). They are generally associated with the plasma membrane, where

they act as molecular scaffolds to bind membrane-associated receptors to intracellular

signaling molecules (15). CARMA1 contains an N-terminal CARD, followed by a

coiled-coil (CC) domain, a PDZ domain, an SH3 domain, and a C-terminal GUK domain,

each of which is critical for its signaling function (33, 56). CARMA1 is constitutively

associated with lipid rafts (19) and it binds directly to Bcl10 through a CARD-CARD

interaction, facilitating recruitment of Bcl10 to lipid rafts upon T cell activation (6, 19, 20,

56). CARMA1 has also been shown to recruit MALT1 to the IS following TCR ligation

(9). Several lines of evidence, then, point to Bcl10, MALT1, and CARMA1 as forming a

trimeric complex immediately downstream of PKCθ in the TCR-induced NF-κB pathway

(*Figure 10*).

Figure 10.
Schematic of CARMA1

Activation of the IKK complex

Recently, the trimeric complex of Bcl10, MALT1, and CARMA1 has been shown

to activate the IKK complex. Oligomers of Bcl10/MALT1 bind to the TRAF6 ubiquitin

ligase via two C-terminal sites on MALT1 (79). The consequent oligomerization of

TRAF6 is believed to facilitate the association of TRAF6 with a complex containing the

ubiquitin-conjugating enzymes Ubc13 and Mms2 (Uev1A) (11, 25). CARMA1 binds

directly to IKKγ/NEMO, perhaps serving as a molecular scaffold to bring the

Bcl10/MALT1/TRAF6 protein complex within biochemical proximity of the IKK

complex (74). Caspase 8 also appears to participate as a bridging enzyme that facilitates

the interaction between IKK and Bcl10/MALT1/TRAF6 (77). Once these two protein

complexes are brought together, TRAF6 K63-polyubiquitinates IKKγ/NEMO. By an

incompletely defined mechanism, this modification of IKKγ/NEMO allows the TAK1

protein kinase to phosphorylate IKKα and IKKβ (79). It is hypothesized that Bcl10

serves to regulate the entire downstream process leading to IKK complex activation (99),

although it is still not understood precisely how Bcl10 is activated by upstream signals

(*Figure 11*).
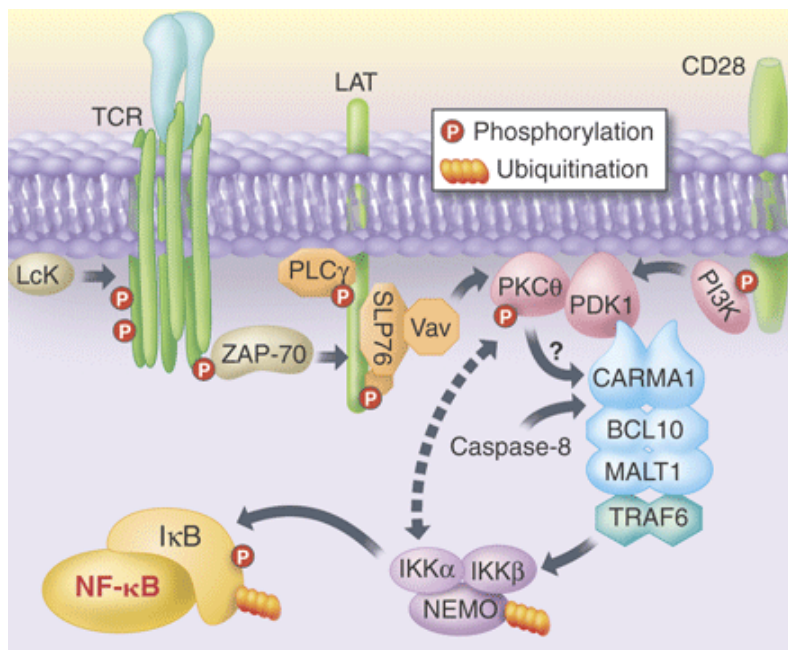
Figure 11. Activation of the IKK complex
Following TCR ligation and the initial tyrosine phosphorylation cascade, PKCθ is recruited to the plasma membrane. By an unknown mechanism, PKCθ activates Bcl10, which results in the assembly of a CARMA1-Bcl10-MALT1-TRAF6 complex. CARMA1 recruits the IKK complex and, in a caspase 8-dependent manner, TRAF6 polyubiquitinates NEMO, leading to the activation of the IKK complex.
(van Oers et al. 2005. *Science 308:65*)

Summary of the TCR-to-NF-κB signaling pathway

The TCR-to-NF-κB signaling pathway, as it is currently understood, can be

summed up as follows. TCR ligation by peptide/MHC leads to an initial tyrosine

phosphorylation cascade that recruits PDK1 and Vav1 to the immunological synapse.

PKCθ is subsequently recruited to the IS, where it is activated, and may stimulate RIP2 to

phosphorylate and activate Bcl10 (although this portion of the pathway remains quite speculative). Bcl10 oligomerizes and binds to MALT1, inducing MALT1 oligomerization. Some data suggest that CARMA1 recruits Bcl10/MALT1 to the IS, while the TRAF6 ubiquitinating complex binds to MALT1. In this model, CARMA1 also recruits the IKK complex to the IS by binding to IKKγ/NEMO. In another (not necessarily mutually exclusive) model, these molecular clustering events occur within discrete cytoplasmic foci, called POLKADOTS (57, 66), which will be discussed in detail below. Subsequent to these molecular clusterings of Bcl10, MALT1, CARMA1, and TRAF6, TRAF6 polyubiquitinates IKKγ/NEMO, probably in a caspase 8 dependent manner. Polyubiquitination of IKKγ/NEMO allows TAK1 to phosphorylate IKKα and IKKβ. Activated IKKβ then phosphorylates IκB, targeting it for ubiquitination and destruction by the 26S proteasome. Destruction of IκB unmasks a nuclear localization signal, allowing NF-κB to translocate to the nucleus where it binds to numerous gene promoters, stimulating transcription (*Figure 12*).
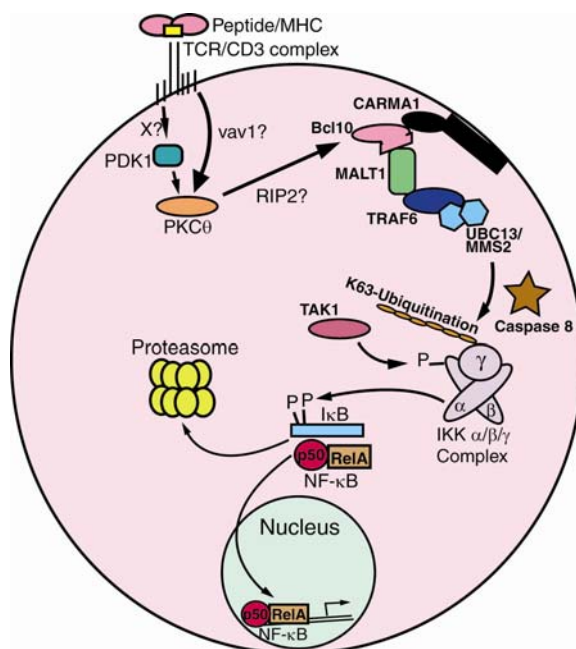
Figure 12. Summary of the TCR-to-NF-κB pathway

Antigen/MHC ligation of the TCR leads to the activation of PKCθ, through an intermediate step involving PDK1 and, possibly, Vav1. PKCθ signaling leads to activation of a complex containing CARMA1, Bcl10, MALT1, and TRAF6. The CARD-containing kinase, RIP2 may phosphorylate Bcl10, thereby activating the Bcl10 signaling complex. In a caspase 8-dependent manner, the TRAF6 ubiquitin ligase and the UBC13/MMS2 ubiquitin conjugating enzymes activate the IKK complex via K63-ubiquitination of IKKγ. This leads to TAK1 phosphorylation of IKKα and IKKβ. Activated IKKβ phosphorylates IκB, leading to subsequent IκB proteolysis. NF-κB is freed to translocate to the nucleus and bind promoter sequences activating transcription. The symbol X? indicates potential unknown intermediates. (Schaefer, 2005)

Previous studies

Previously, the principal investigator (PI) of this laboratory (66) sought to further elucidate the molecular interactions at the c-SMAC of the IS following T cell activation *in vivo*. Using primarily molecular imaging as a means of studying stimulated T cells, he was able to demonstrate a complex relocalization of NF-κB signaling intermediates to the c-SMAC. Molecular imaging methodology involves the use of fluorescently-tagged proteins or fluorescently-labeled antibodies to examine protein localization within cells using powerful and sophisticated microscopy. Molecular imaging has been used successfully in the past to observe redistribution of T cell signaling intermediates at a subcellular level (19, 49, 50), with the unique power of this approach being that signal transduction can be observed within individual cells of a population (63). Biochemical methods of elucidating signal transduction mechanisms require bulk cultures of cells and, hence, cannot completely describe protein redistribution events (66).

The PI demonstrated that, upon T cell activation by APCs, PKCθ translocates to the developing c-SMAC. Within several minutes, PKCθ reaches maximal enrichment at this site and then begins to slowly reverse. Concurrent with maximal enrichment of PKCθ at the c-SMAC, Bcl10 oligomerizes into punctuate and filamentous structures throughout the cytoplasm. These structures were termed punctuate and oligomeric killing or activating domains transducing signals (POLKADOTS), because of their physical and functional (i.e., signal transduction) similarity to death effector filaments formed by specific mediators of apoptosis (71) *(Figure 13)*. The Bcl10 POLKADOTS then migrate to and become enriched at the c-SMAC. Also, Bcl10 POLKADOTS formation and Bcl10 phosphorylation are abrogated by blocking PKCθ activation (66). From these data,

the PI hypothesized that early PKCθ activation of Bcl10 occurs in the cytoplasm, but that

long-term stable signaling, which is required for continued T cell activation, may occur at

the mature c-SMAC (10, 66). Also, he hypothesized that Bcl10 POLKADOTS are

functionally significant in NF-κB activation. Finally, the PI demonstrated the validity of

his molecular imaging approach and showed that fluorescently-tagged proteins behave

similarly to endogenous proteins *in vivo*.

A

B

APC

APC

No Antigen

+Conalbumin (specific antigen)

Figure13. Bcl10 forms POLKADOTS upon T cell activation
A. D10 T cells expressing Bcl10-GFP are conjugated to CH12 B cells (APC) in the absence of antigen. Bcl10 remains diffuse throughout the cell cytoplasm. B. Conalbumin-loaded APCs activate D10 T cells expressing Bcl10-GFP. Bcl10 relocalizes into punctuate and filamentous structures. (Schaefer et al. 2004. *PNAS 101:1004*)

Recently, a report from this laboratory was published that demonstrates the

functional importance of Bcl10 POLKADOTS in NF-κB activation (57). Utilizing a

combination of methodologies (molecular imaging, FRET analysis, and biochemistry) to

examine the nature of POLKADOTS, these structures were shown to form only under

conditions that permit NF-κB activation. Also, POLKADOTS were shown to be

enriched with Bcl10 oligomers and Bcl10 in close association with various signaling

partners, including MALT1, RIP2, CARMA1, and TRAF6. From these data we

proposed a model for POLKADOTS structure and function, whereby POLKADOTS

contain tightly packed oligomers of Bcl10 and MALT1 that interact with other partner

proteins at the exposed surfaces of the structures. These protein clusters may serve as

focal sites of dynamic information exchange between signaling intermediates of the NF-κB pathway (57).

Specific Aims of this study

Building on the previous work of this laboratory, the purpose of this study was to further elucidate the regulation of protein-protein associations by signaling intermediates in the TCR-to-NF-κB pathway. This study proposed to specifically characterize the molecular mechanisms of Bcl10-regulated interactions with its partner signaling proteins. The study combined mutational analysis, molecular imaging, biochemistry, and computer/bioinformatics modeling to completely describe the scientific findings.

Aim 1. To precisely define the binding site for MALT1 to Bcl10

A putative binding site for MALT1 is believed to be located immediately downstream of the N-terminal CARD of Bcl10 (46). While MALT1 may bind in this general vicinity, the amino acid residues essential for binding have not been identified. *We hypothesize that the MALT1 binding site extends upstream into helix 6 of the Bcl10 CARD, and it includes at least a portion of the binding domain that has been previously characterized.*

Aim 2. To map the N-terminal functional domains of Bcl10

Several CARD proteins have been reported to interact with the Bcl10 CARD to activate NF-κB (e.g., CARD9, CARD10, CARMA1, CARD14, RIP2, and BinCARD) (5, 6, 20, 47, 56, 59, 94). Although CARDs have generally been thought of as domains mediating only CARD-CARD interactions, a recent report has demonstrated that CARDs are capable of binding non-CARD proteins (51). The Bcl10 CARD has three potential binding faces, each comprised of two helices. No binding partners have yet been

identified for the helix 5/6 face of any CARD protein. Additionally, there is no information regarding which helical faces of Bcl10 are involved in interactions with its partner CARD proteins. *We hypothesize that the helix 5/6 face of the Bcl10 CARD is a site of heterotypic (CARD-non-CARD) interaction with MALT1 and, possibly, also a site of homotypic (CARD-CARD) interaction with one or more CARD-containing binding partners of Bcl10.*

Aim 3. To determine the function of the C-terminus of Bcl10

Bcl10 has not yet been crystallized, so its complete structure is unknown. While it possesses an N-terminal CARD based on sequence homology, its C-terminus is of unknown structure and function. *We hypothesize that the C-terminus plays an important role in the regulation of the ability of Bcl10 to activate NF-κB.*

Significance of this work

By understanding the mechanistic relationships between Bcl10 and its partner signaling proteins, new knowledge can be gained about Bcl10 regulation of the TCR-to-NF-κB pathway. This study consists of a detailed structure/function analysis of Bcl10 that provides further information defining the regulatory domains of this key T cell signaling intermediate. These data can be used to gain general insight into how protein interactions within signal transduction cascades are regulated. Finally, the TCR-to-NF-κB signaling pathway plays an important role in the pathogenesis of MALT lymphoma. A thorough understanding of this signaling cascade may lead to the development of drugs that can disrupt the signaling pathway at the level of a single molecular intermediate. Such drugs could provide useful therapies for diverse pathologies including MALT lymphoma, autoimmunity, and organ transplant rejection.

Chapter 2. Research Design

Aim 1. To precisely define the binding site for MALT1 to Bcl10

A putative binding site for MALT1 is believed to be located immediately downstream of the N-terminal CARD of Bcl10 (46). While MALT1 may bind in this general vicinity, the amino acid residues essential for binding have not been identified. *We hypothesize that the MALT1 binding site extends upstream into helix 6 of the Bcl10 CARD, and it includes at least a portion of the binding domain that has been previously characterized.*

Rationale (Aim 1)

Mutational analysis and subsequent biochemical analysis are standard experimental approaches for studying the molecular basis of protein function. Other methods of protein evaluation include reporter assays, molecular imaging, and computer/bioinformatics modeling of potential functional domains. Taken together, the data derived from such experimental analyses would be expected to yield a significant amount of knowledge about the structure and function of Bcl10. These data could then be used to support the data gained from a crystallized Bcl10. Currently, this lab is collaborating with Drs. Sangwoo Cho and Roy Mariuzza at the University of Maryland Center for Advanced Research in Biotechnology (CARB) to generate a Bcl10-MALT1 co-crystal and to determine precisely how these two molecules interact.

For the experiments in this Aim, the methods above were used to study Bcl10 in a systematic way. Heavy emphasis was placed on Bcl10 amino acid mutation (point mutation and deletion) as a means of disrupting normal Bcl10 function. By observing the

altered phenotype of mutated Bcl10, inferences about Bcl10's normal structure and functional interactions with other proteins were made.

Experimental Design (Aim 1)

Bcl10 mutagenesis

In this Aim, Bcl10 mutations encompassed the putative MALT1 binding domain (amino acids (aa) 107-119) (46) and a region immediately upstream of this domain. PCR site-directed mutagenesis is a commonly used method of generating amino acid mutations in cDNA. This method proved to be a straightforward and relatively rapid way of generating both point mutations and deletion mutations. In the case of point mutations, only inter-species conserved residues were targeted for mutation and the type of mutation was intended to alter the biochemical properties of the wild-type residue. For example, hydrophobic residues were changed to the polar lysine (K) and charged residues were changed to the uncharged alanine (A). All Bcl10 mutant cDNAs were cloned into a murine stem cell virus (MSCV) cloning vector for ease of assembly and sequence verification. An added feature of the MSCV vector used was the presence of a GFP gene fused to the C-terminus of the Bcl10 gene. Hence, this plasmid encoded a Bcl10-GFP fusion protein that could be directly visualized by epifluorescent microscopy. Most Bcl10 mutant cDNAs were then subcloned into a Moloney murine leukemia virus (MMLV) retroviral vector, which also includes a G418-selectable marker, to facilitate the production of stable T cell lines and follow-on biochemical experiments.

T cell microscopy

The T cell line used in this Aim, D10 (described in Methods), has a TCR that recognizes conalbumin peptide in the context of MHC H-2^k. For this reason, the APCs

used to activate D10 T cells were conalbumin-loaded CH12 H-2^k-positive B cells. Once

retroviral plasmids encoding mutant forms of Bcl10-GFP had been generated, they were

used to stably infect D10 T cell lines. Mutant D10 T cells were first evaluated for their

ability to express GFP by fluorescence-activated cell sorting (FACS) analysis. The

degree to which the cells expressed GFP gave an indication of the efficiency of mutant

Bcl10 expression and, we believe, the expression levels also provided some insight into

whether the Bcl10 mutant was influencing D10 cellular physiology. Mutant D10 T cell

clones were conjugated to CH12 B cells in order to provide the most physiological form

of antigen stimulation to the T cell. Once T cells were activated by antigen, they were

examined for POLKADOTS microscopically. With this approach, we were able to infer

changes in the interaction between Bcl10 and MALT1 by observing changes to the

expected phenotype of POLKADOTS formation.

Immunoblotting

Western blotting (immunoblotting) was used as the readout for most of the

biochemical experiments in this Aim. Following the cellular expression of Bcl10 mutant

proteins and their testing within the context of a given experiment, proteins recovered

from cell lysates were electrophoretically separated on a denaturing polyacrylamide gel

(SDS-PAGE). Using this method, proteins were separated by molecular size and

detected with specific antibodies. Bcl10-GFP is a relatively large protein (60kDa) and

can be detected using one of the many Bcl10 antibodies that have been generated

specifically for this purpose.

Calcium-phosphate transfection

For each of the biochemical experiments used in this Aim, Bcl10 mutants were transiently transfected into HEK-293T cells. This cell line was particularly conducive to transfection using a modification of a calcium phosphate method (32). The purpose of transfection was to introduce large amounts of foreign DNA into the cell line to transiently induce high levels of expression of the encoded genes. The 293T cells were used in lieu of D10 T cells because much higher levels of expression could be achieved in 293T cells, enabling biochemical analysis.

Bcl10-CARMA1 co-transfection assay

To demonstrate that the mutations made in the Bcl10 CARD did not affect the structure and function of the CARD, 293T cells were co-transfected with mutant Bcl10-GFP and CARMA1. If a given Bcl10 mutation were to result in an improperly folded CARD, then a mutant phenotype that appeared to impair MALT1 binding might actually be the result of a damaged CARD. Bcl10 phosphorylation has been shown to result from its functional interaction with CARMA1 through its CARD (20). In this assay, Bcl10 phosphorylation, subsequent to CARMA1 interaction, was evaluated by recovering the 293T cell lysates, separating the proteins by SDS-PAGE, and probing the blots for the presence of phosphorylated Bcl10.

Bcl10-MALT1 co-immunoprecipitation assay

Co-immunoprecipitation was used to assess the relative ability of various Bcl10 mutants to interact with MALT1. A given mutation was determined to be in the MALT1 binding domain if mutant Bcl10 could no longer complex with MALT1 compared to wild-type Bcl10 and if it was determined to have an intact, properly folded CARD via the

CARMA1 co-transfection assay. Following co-transfection of 293T cells with 3xHA-tagged mutant Bcl10-GFP and FLAG-tagged MALT1-ΔC (aa 2-344), cell lysates were recovered and subjected to a modified co-immunoprecipitation method (24). Only the N-terminus of MALT1 was used in these experiments, since the N-terminus contains the two Ig-like domains that interact with Bcl10 and since this truncated MALT1 protein can be expressed at much higher levels than the full-length MALT1. Bcl10-MALT1 protein complexes were captured using an antibody to FLAG and recovered on Protein G sepharose. The co-immunoprecipitated proteins were denatured, separated by SDS-PAGE, and identified by immunoblot using an antibody to the 3xHA epitope tag.

NF-κB luciferase reporter assay

Following co-transfection of 293T cells with mutant Bcl10-GFP and NF-κB luciferase assay reporter vectors (described in Methods), cell lysates were recovered and subjected to a luciferase assay and accompanying β-galactosidase assay (Promega). The luciferase assay was used to measure the relative NF-κB activity of the Bcl10 mutants, while the β-galactosidase assay was used to measure the relative efficiency of transfection, thus serving as an internal control. If a given mutation abrogated NF-κB activity, then the interpretation would be that either the mutation had impaired the ability of Bcl10 to bind to MALT1 or the mutation had altered the overall structure of Bcl10, such that the protein was no longer properly folded. The CARMA1 co-transfection assay, examining the functional interaction between Bcl10 and CARMA1, was used to discriminate between these two possibilities. Bcl10 mutants that abrogated NF-κB activity, but could still interact with CARMA1 (as assessed by Bcl10 phosphorylation), were interpreted to be mutations that impaired the ability of Bcl10 to bind to MALT1. In

contrast, mutations that abrogated both NF-κB activation and CARMA1-dependent Bcl10 phosphorylation, were interpreted to be mutations that disrupted the folding of the Bcl10 CARD.

Taken together, the T cell POLKADOTS imaging, the CARMA1 co-transfection assay, the MALT1 co-immunoprecipitation assay, and the NF-κB luciferase assay, provided strong data indicating which amino acids of Bcl10 are critical for MALT1 binding and Bcl10-mediated NF-κB activation.

Aim 2. To map the N-terminal functional domains of Bcl10

Several CARD proteins have been reported to interact with the Bcl10 CARD to activate NF-κB (e.g., CARD9, CARD10, CARMA1, CARD14, RIP2, and BinCARD) (5, 6, 20, 47, 56, 59, 94). Although CARDs have generally been thought of as domains mediating only CARD-CARD interactions, a recent report has demonstrated that CARDs are capable of binding non-CARD proteins (51). The Bcl10 CARD has three potential binding faces, each comprised of two helices. No binding partners have yet been identified for the helix 5/6 face of any CARD protein. Additionally, there is no information regarding which helical faces of Bcl10 are involved in interactions with its partner CARD proteins. *We hypothesize that the helix 5/6 face of the Bcl10 CARD is a site of heterotypic (CARD-non-CARD) interaction with MALT1 and, possibly, also a site of homotypic (CARD-CARD) interaction with one or more CARD-containing binding partners of Bcl10.*

Rationale (Aim 2)

The experimental rationale for this Aim is very similar to that described in Aim 1. Mutational analysis, biochemical examination, and computer/bioinformatics modeling

were used to further elucidate the structure and function of Bcl10. In this Aim, however, molecular imaging was not incorporated because the data derived from this method were felt to be redundant with the data generated in Aim 1 and would, therefore, not significantly extend the knowledge of Bcl10 biology.

Experimental Design (Aim 2)

Computer modeling and Bcl10 mutagenesis

In this Aim, a computer threading model (40) was used to generate a structure for the Bcl10 CARD based upon previous X-ray crystallographic data of the structure of the APAF-1 and procaspase-9 CARD domains. This threading model was used to predict the positions of solvent-exposed amino acid residues in the Bcl10 CARD. This computer model was evaluated against the experimental evidence to determine precisely where MALT1 binds to Bcl10. Also, Bcl10 mutations were restricted to the helices 5/6 of the Bcl10 CARD, as predicted by the computer threading model. As in Aim 1, PCR site-directed mutagenesis was used to generate Bcl10 mutant cDNAs which were cloned into the MSCV vector. Only Bcl10 point mutants (no deletion mutants) were generated for this Aim. The MMLV retroviral vector was not used in this Aim because D10 T cell infections for molecular imaging were not needed. Also, for this reason, FACS analysis to determine GFP expression was not used.

Co-immunoprecipitation, CARMA1 co-transfection assay, and NF-κB luciferase assay

Immunoblotting continued to be an important method for visualizing the mutant Bcl10 proteins following biochemical manipulation. Co-immunoprecipitation was used to determine which mutations impaired the binding between Bcl10 and partner proteins. The CARMA1 co-transfection assay was used to determine which mutations disrupted

proper folding of the Bcl10 CARD. And the NF-κB luciferase assay was used to determine whether mutations that abrogate Bcl10-partner protein interactions also abrogate NF-κB activation.

Taken together, these experiments identified which amino acids were necessary for Bcl10 CARD interaction with partner proteins. To some degree, these studies also allowed for verification and refinement of the computer-predicted model of the helix 5/6 region of the Bcl10 CARD.

Aim 3. To determine the function of the C-terminus of Bcl10

Bcl10 has not yet been crystallized, so its complete structure is unknown. While it possesses an N-terminal CARD based on sequence homology, its C-terminus is of unknown structure and function. *We hypothesize that the C-terminus plays an important role in the regulation of the ability of Bcl10 to activate NF-κB.*

Rationale (Aim 3)

As in Aims 1 and 2, Bcl10 structure and function were examined via creation and analysis of Bcl10 mutants. In this Aim, mutational analysis, biochemical examination, and molecular imaging were used to gain information about the C-terminus of Bcl10. Currently, there are no proteins that are known to interact with the Bcl10 C-terminus, therefore, co-immunoprecipitation experiments were not performed. Also, since bioinformatics approaches have identified no conserved domains in Bcl10, C-terminus computer modeling could not be used to gain insight into the possible structure of this large region.

Experimental Design (Aim 3)

Bcl10 mutagenesis and T cell microscopy

In this Aim, Bcl10 mutants were generated that collectively spanned the entire C-terminus downstream of the Bcl10 CARD, including the putative MALT1 binding site (46). As in Aims 1 and 2, PCR site-directed mutagenesis was used to generate Bcl10 mutant cDNAs which were cloned into the MSCV vector. Only Bcl10 deletion mutants were generated for this Aim. Also, Bcl10 mutant cDNAs were subcloned into MMLV retroviral vectors for D10 T cell infection and subsequent fluorecence imaging.

Bcl10 phosphorylation assay and NF-κB luciferase assay

Immunoblotting was used to visualize the results of Bcl10 phosphorylation experiments performed for this Aim. Bcl10 phosphorylation is believed to be an indicator of NF-κB activation and the C-terminus of Bcl10 is capable of being phosphorylated (59, 66) (and the work described herein). Because Bcl10 phosphorylation has been shown to be the result of functional interaction with CARMA1 (20), phosphorylation of Bcl10 may play a role in Bcl10-mediated signal transduction. To determine whether the C-terminus regulates the activity of Bcl10, progressive Bcl10 C-terminal truncations were generated and tested for their ability to be phosphorylated in D10 T cells. Mutant Bcl10 D10 T cells were stimulated *in vitro* by cross-linking their TCRs with immobilized anti-TCR (αTCR) antibody in six-well plates. Following a 1 hr incubation in these plates, D10 T cell lysates were recovered, proteins were separated by SDS-PAGE, and blots were probed for the presence of phosphorylated Bcl10.

The results of these experiments provided important information about how Bcl10 phosphorylation is regulated. The NF-κB luciferase assay was also used to test the relative NF-κB activation potential of each of the Bcl10 deletion mutants.

Chapter 3. Experimental Results

Deletion of the MALT1 binding domain of Bcl10 abrogates POLKADOTS

formation

We began our structural/functional study of Bcl10 by deleting the MALT1

binding site (amino acids 107-119) as described by Lucas, *et al* (46) *(Figure 14)*. We

generated a Bcl10 wild-type (WT) plasmid construct fused to GFP at its C-terminus and,

using PCR site-directed mutagenesis, we made a Bcl10-ΔMALT1 plasmid construct

(which deletes the previously defined minimal MALT1 binding site, from aa107-119)

also fused to GFP. We predicted that the resulting Bcl10-WT-GFP and Bcl10-ΔMALT1-

GFP fusion proteins would be successfully expressed in T cells based upon our previous

work with similar Bcl10-fluorescent protein fusions (66). We stably infected a D10 T

cell line with either Bcl10-WT-GFP or Bcl10-ΔMALT1-GFP, stimulated the cells in the

presence of conalbumin-loaded CH12 B cells, and observed the cells using epifluorescent

microscopy. For the Bcl10-WT-GFP D10 T cells, we observed the expected

POLKADOTS pattern typical of Bcl10 oligomerization following antigen stimulation

(66). Similarly, Bcl10-WT-GFP T cells that were not activated with antigen

demonstrated a diffuse GFP pattern indicative of inactive Bcl10 that had not undergone

oligomerization (66). For the Bcl10-ΔMALT1-GFP D10 T cells, we observed a diffuse

GFP pattern both with and without antigen stimulation. This phenotype was also

expected in light of our recent findings that Bcl10 oligomerization occurs cooperatively

with MALT1 oligomerization (57). In the Bcl10-ΔMALT1-GFP D10 T cells, MALT1

could no longer bind to Bcl10 and, hence, could not influence Bcl10 oligomerization

(Figure 15).

CARD

MEAPAPSLTEEDLTEVKKDALENLRVYLCEKIIAERHFDHLRAKKILSREDTEEISCRTSSRKRAGKLLDY

```
10        20        30        40        50        60        70
          Helix 1             Helix 2        Helix 3        Helix 4
```

LQENPRGLDTLVESIRREKTQSFLIQKITDEVLKLRNIKLEHLKGLKCSSCEPFAAGATNNLSRCNSDESN

```
80        90        100       110       120       130       140
      Helix 5          Helix 6   Minimal MALT1 interaction motif
```

LSEKQRASTVMYHPEGESSTAPFFSMASSLNLPVLEVGRTENSSFSSATLPRPGDPGAPPLPPDLRLEEGG

```
150       160       170       180       190       200       210
```

SCGNSSEMFLPLRSRALSRQ

```
220       230
```

Figure 14. Bcl10 functional domains
      This is a representation of the Bcl10 gene and its functional domains as they are currently understood: an N-terminal CARD based on homology studies, a 13 amino acid MALT1 binding domain as described by Lucas, *et al* (46), and a C-terminus of unknown function that can be phosphorylated.
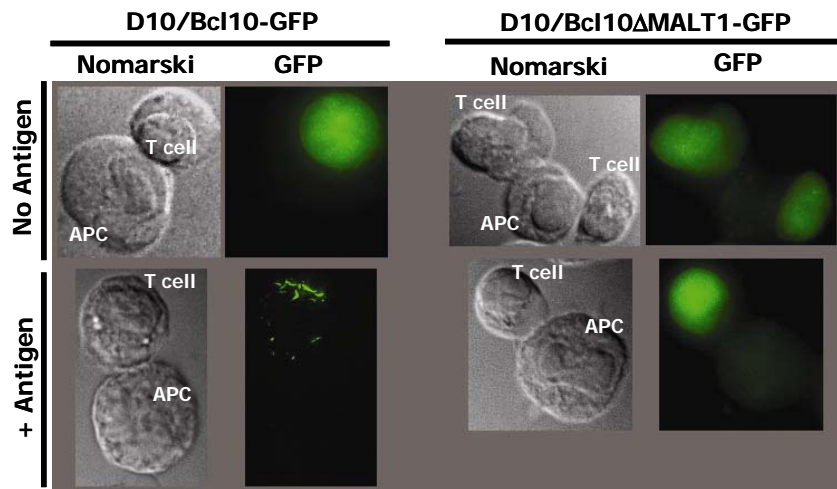
Figure 15. MALT1 binding to Bcl10 is required for POLKADOTS formation
      D10 T cells expressing Bcl10-WT-GFP were conjugated to CH12 B cells in the absence or presence of 250µg/ml conalbumin (Antigen) and imaged via wide-field fluorescence microscopy. These D10 T cells were observed to form Bcl10 POLKADOTS upon activation. D10 T cells expressing Bcl10-ΔMALT1-GFP were similarly activated and imaged. These activated D10 T cells failed to form Bcl10 POLKADOTS. (Rossman et al. 2006. *MBC*)

      We wanted to assure ourselves that the absence of POLKADOTS in Bcl10-

ΔMALT1-GFP D10 T cells was not due to a lower expression of the mutant, relative to

the wild-type. We FACS sorted Bcl10-WT-GFP D10 T cells and identified a subclone (Bcl10-WT-GFP-Dull) with low uniform expression of Bcl10-WT-GFP that was comparable to the expression level in the Bcl10-ΔMALT1-GFP cell line. When we activated these cells with antigen, we observed faint POLKADOTS consistent with the lower expression of the GFP fusion protein. Hence, fusion protein expression levels do not influence POLKADOTS formation (*data not shown*).

The downstream amino acids of the MALT1 binding domain of Bcl10 are not critical for POLKADOTS formation

To isolate the amino acids essential for MALT1 binding to Bcl10, we made point mutations of inter-species conserved amino acid residues within and immediately upstream of the MALT1 binding region (*Table 1*). For these experiments, we generated single or multiple amino acid point mutants of Bcl10. We substituted charged residues with alanine (A) and hydrophobic residues with lysine (K) in expectation of disrupting protein-protein interactions at the site of each mutation. These mutations included conserved residues of Bcl10, spanning aa105 to aa117.

minimal MALT1 binding site
(as previously defined)

	105		107		109		111		113		115		117		119
Mouse	K	L	R	N	I	K	L	E	H	L	K	G	L	K	C
Human	K	L	R	N	I	K	L	E	H	L	K	G	L	K	C
Rat	K	L	R	N	I	K	L	E	H	L	K	G	L	K	C
Chicken	K	V	K	N	E	K	L	E	A	L	K	G	L	S	C
Fugu	K	A	K	N	E	K	I	E	T	L	K	A	A	A	S
Consensus	K	L/V/A	R/K	N	X	K	L/I	E	X	L	K	G/A	L/A	X	X
K105A	A														
L106K		K													
R107A			A												
N108A				A											
K110A						A									
L111K							K								
EH112,113AA								A	A						
L114K										K					
K115A											A				
G116K												K			
L117K													K		
KKK105,110,115AAA	A					A					A				
LLL106,111,114KKK		K					K			K					

Table 1. MALT1 binding site mutations alignment
The inter-species conserved residues aa105-119 are represented, with the consensus sequence below. An X indicates no consensus at that position. Listed below are each of the Bcl10 point mutants we generated for this region, with the specific amino acid substitution(s) indicated.

Following generation of clonal D10 T cell lines with these constructs, we stimulated the cells in the presence of CH12 B cells as described above. We identified three Bcl10 point mutants that could not form POLKADOTS upon T cell activation: L106K, LLL106,111,114KKK (LLL>KKK), and KKK105,110,115AAA (KKK>AAA). We felt that the negative POLKADOTS phenotype for the LLL>KKK mutant was likely due to the L106K mutation, but that the KKK>AAA negative POLKADOTS phenotype could not be accounted for by a single point mutation. It was interesting to us that no single point mutation in the aa107-119 MALT1 binding region resulted in a negative

POLKADOTS phenotype. Also, now we had identified one mutation (L106K) upstream

of the putative MALT1 binding site that failed to form POLKADOTS (*Table 2*).

Bcl10-GFP Construct	NF-κB Activation	POLKADOTS formation
WT	++++	Y
dMALT1	-	N
K105A	+++	Y
L106K	-	*N
R107A	++++	Y
N108A	++++	Y
K110A	+	Y
L111K	++	Y
EH112.113AA	++	Y
L114K	++++	Y
K115A	++	Y
G116K	++++	Y
L117K	++++	Y
KKK105,110,115AAA	-	N
LLL106,111,114KKK	-	N

++++, >75% WT activation
+++, 50% - 75% WT activation
++, 25% - 50% WT activation
+, 10% - 25% WT activation
-, Less than 10% WT activation
Y, yes; N, no; NE, not examined
*Indicates a minority population of cells with POLKADOTS that are smaller and less intense than WT

Table 2. Few residues in the MALT1 binding site are required for POLKADOTS formation
    D10 T cells expressing Bcl10-GFP constructs were conjugated to APCs bearing 250μg/ml conalbumin and imaged by fluorescence microscopy. Bcl10 POLKADOTS formation was scored Y or N on the basis of an overwhelming majority of cells observed in a field of 20 or more conjugating pairs.

POLKADOTS formation correlates with NF-κB activation by MALT1 binding

domain mutants of Bcl10

Next we wanted to see if our microscopic POLKADOTS findings correlated with

NF-κB activation. We transiently transfected Bcl10-WT-GFP, Bcl10-ΔMALT1-GFP,

and the collection of Bcl10-GFP point mutants into 293T cells along with an NF-κB

luciferase reporter vector system. Although Bcl10 is endogenously expressed in 293T

cells, we expected our overexpressed constructs to preferentially influence the 293T

cells' endogenous signaling machinery. Also, consistent with previously published data

(46), we observed that overexpression of functional Bcl10 is sufficient to stimulate NF-κB activation in the absence of a receptor-generated signal, presumably due to overexpression-induced Bcl10 oligomerization. We found that, relative to NF-κB activation of Bcl10-WT, NF-κB activation for Bcl10-ΔMALT1, -L106K, -LLL>KKK, and –KKK>AAA were nearly undetectable. The remaining Bcl10 point mutants, on the other hand, were able to activate NF-κB, to varying degrees (*Figure 18*). These findings were consistent with our observations that Bcl10-ΔMALT1, -L106K, -LLL>KKK, and –KKK>AAA could not form POLKADOTS subsequent to T cell activation, while Bcl10-WT and the remaining Bcl10 point mutants could form POLKADOTS (*Table 2*). These data were further evidence of the strong correlation between NF-κB activation and POLKADOTS formation.

Regarding the unusual KKK>AAA phenotype, we observed that the individual mutations of K105A, K110A, and K115A resulted in a slight reduction in NF-κB activation, but that the additive effect of the mutation of the three lysines together completely abrogated NF-κB activation *(Figure 16)*. Perhaps the structure of Bcl10 in this region makes the charges of three lysines collectively important, but not individually important.

To assure ourselves that the level of Bcl10 protein overexpression in the 293T cells was not influencing the degree of NF-κB activation, we immunoblotted cellular lysates and probed for the presence of Bcl10. We found that Bcl10 expression by immunoblot did not correlate with changes in NF-κB activation by luciferase assay. Hence, protein expression level does not account for differences in NF-κB activation by these mutants (*data not shown*).
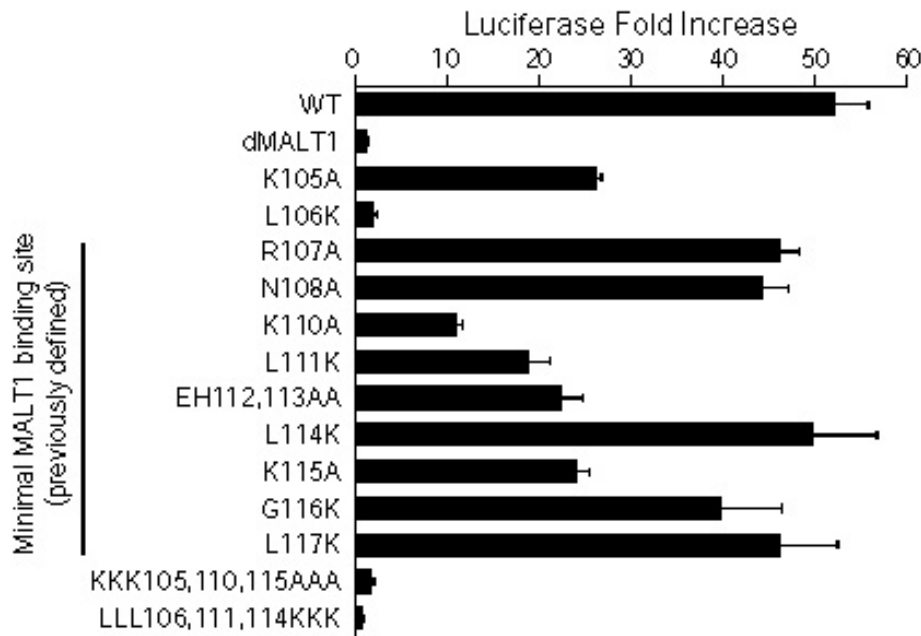
Figure 16. Few residues in the MALT1 binding domain are required for NF-κB activation
293T cells were transiently transfected with a Bcl10-construct and NF-κB luciferase assay reporter vectors. After 48 hrs, cell lysates were recovered and assayed for NF-κB activation as measured by fold luciferase increase relative to reporter vector, alone and transfection efficiency. Relative to the Bcl10-WT positive control and the Bcl10-dMALT1 negative control, three null Bcl10 mutants were identified: L106K, KKK>AAA, and LLL>KKK. Each Bcl10-construct was assayed in triplicate and error bars represent the standard deviation.

Only the upstream portion of the MALT1 binding domain is critical for

POLKADOTS formation and NF-κB activation

To confirm that the downstream amino acids of the MALT1 binding domain are not critical for POLKADOTS formation and NF-κB activation, we made progressive deletions of the MALT1 binding domain. In a manner analogous to the generation of Bcl10-ΔMALT1-GFP, we generated Bcl10-deletion 7 (D7)-GFP, Bcl10-D8-GFP, and Bcl10-D9-GFP. D7 truncated Bcl10 at amino acid 118, D8 at amino acid 114, and D9 at amino acid 106 (*Figure 17*). The D7-D9 designation accounted for previous deletions (D1-D6) of the C-terminus made in our lab, which will be discussed later in this chapter. Also, D9 was equivalent to a construct that was previously shown not to bind to MALT1 (46).
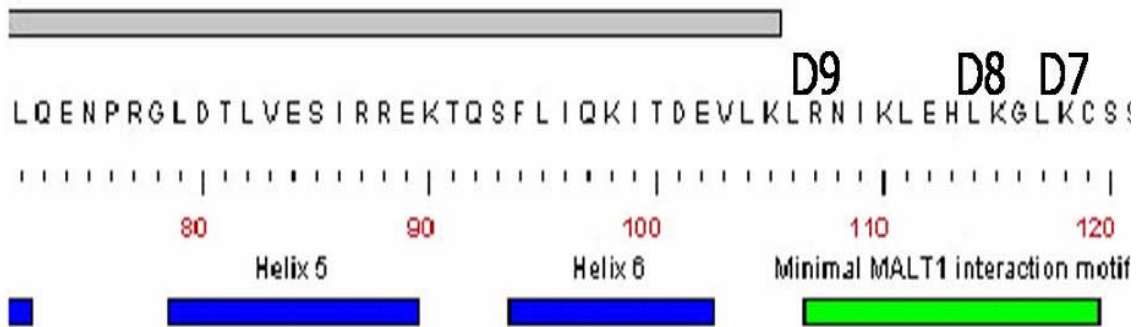
Figure 17. MALT1 binding domain deletions
 D7 truncated Bcl10 at amino acid 118, D8 at amino acid 114, and D9 at amino acid 106.

We again generated D10 clonal T cell lines with our constructs and observed them microscopically for POLKADOTS following antigen stimulation. Bcl10-D7-GFP and Bcl10-D8-GFP formed POLKADOTS in response to antigen stimulation, while Bcl10-D9-GFP did not. Similarly, we found that, relative to NF-κB activation of Bcl10-WT, NF-κB activation of Bcl10-D7 and –D8 was high, but NF-κB activation of Bcl10-D9 was undetectable (*Figure 18*). Additionally, we co-immunoprecipitated FLAG-tagged MALT1 with 3xHA-tagged Bcl10-WT, -D7, -D8, and –D9. For these experiments, we used a MALT1 N-terminal-only construct that contained the Ig-like domains required for binding to Bcl10, which was highly expressed in 293T cells, and which had been used previously in similar experiments (46). Compared to its interaction with Bcl10-WT, MALT1 was able to interact with D7 and D8 to a similar degree, however, it was unable to interact with D9 at all (*Figure 19*). Hence, because of the tight correlation between POLKADOTS formation and Bcl10-MALT1 interaction (and, to some degree, NF-κB activation), we reasoned that amino acids 107-114 were likely to be critical for MALT1 binding to Bcl10, whereas amino acids 115-119 were likely to be dispensable for MALT1 binding (*Figure 17*).

Luciferase Fold Increase
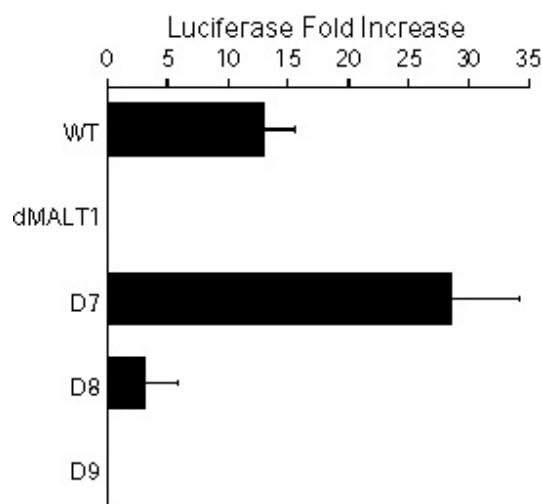
Figure 18. Only a portion of the MALT1 binding domain is critical for NF-κB activation

293T cells were transiently transfected with a Bcl10-construct and NF-κB luciferase assay reporter vectors. After 48 hrs, cell lysates were recovered and assayed for NF-κB activation as measured by fold luciferase increase relative to reporter vector, alone and transfection efficiency. Relative to the Bcl10-WT and Bcl10-dMALT1 control, only Bcl10-D9 failed to activate NF-κB. Each Bcl10-construct was assayed in triplicate and error bars represent the standard deviation.
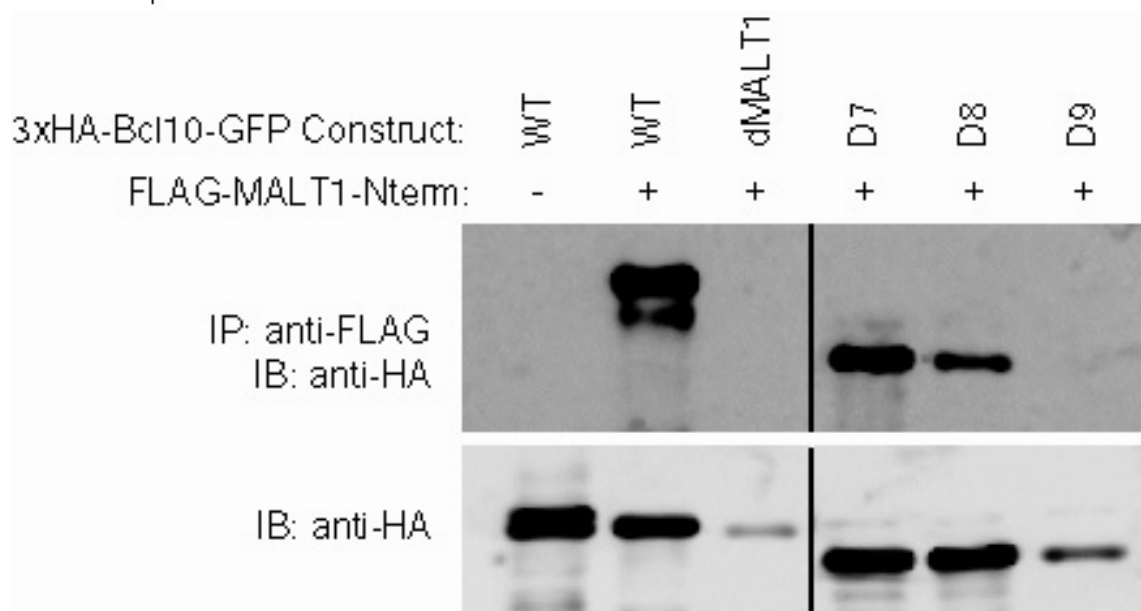
Figure 19. Residues downstream of aa114 are not critical for MALT1 interaction with Bcl10

293T cells were co-transfected with a 3xHA-tagged Bcl10-construct and FLAG-MALT1. After 48 hrs, cell lysates were recovered and subjected to 1μg anti-FLAG antibody capture and 20μl Protein G sepharose recovery. Following protein separation by SDS-PAGE, immunoblots were probed with anti-HA antibody. Bcl10-WT revealed two bands (the upper band being phosphorylated Bcl10). Bcl10-D7 and –D8 interacted strongly with MALT1, while –D9 failed to interact. Based on previous studies, 3xHA-Bcl10 protein expression, as revealed in the anti-HA immunoblot below, did not correlate with the degree of MALT1 interaction.

The helix 5/6 face of the Bcl10 CARD lies adjacent to residues critical for MALT1

binding to Bcl10

Having now identified a significantly smaller amino acid region critical for

MALT1 binding, as well as a critical point mutant (L106K) upstream of this region, we

hypothesized that the remainder of the MALT1 binding domain must lie within the Bcl10 CARD. We based this hypothesis on the knowledge that Ig-like domains typically bind to large patches on target proteins. Hence, a small peptide such as aa107-114 would appear to be too short to accommodate the two Ig-like domains of MALT1. Since we were reasonably certain that binding did not occur downstream of this region, we reasoned that the remainder of the binding site had to be upstream and into the Bcl10 CARD.

We began our study of the Bcl10 CARD by using a computer threading program to generate a predicted 3-dimensional model of the CARD, using the solved crystal structure of procaspase-9 (accession number 3GYS) as the modeling template. The threading program successfully generated a 3-dimensional model of a Bcl10 fragment (aa13-aa110) containing the Bcl10 CARD. Examination of this model revealed the predicted six alpha helices surrounding a hydrophobic core. Using this model, we determined that helix 6 lies immediately adjacent to L106K, one of our null mutants. Also, our predicted model suggested that there are potentially three binding faces of the Bcl10 CARD: helix 1/4, helix 2/3, and helix 5/6 (*Figure 20*). Previous analyses of CARD-CARD interactions based on X-ray crystallographic data have suggested that the helix 1/4 and helix 2/3 faces are involved in such interactions (90). Currently, there are no known examples of protein-protein contacts involving the helix 5/6 face of any CARD protein (although there are very few crystal structures available for analysis). From these observations, we hypothesized that the actual MALT1 binding site might include all or part of the helix 5/6 face. Our next set of Bcl10 mutations thus encompassed the helix 5/6 face.
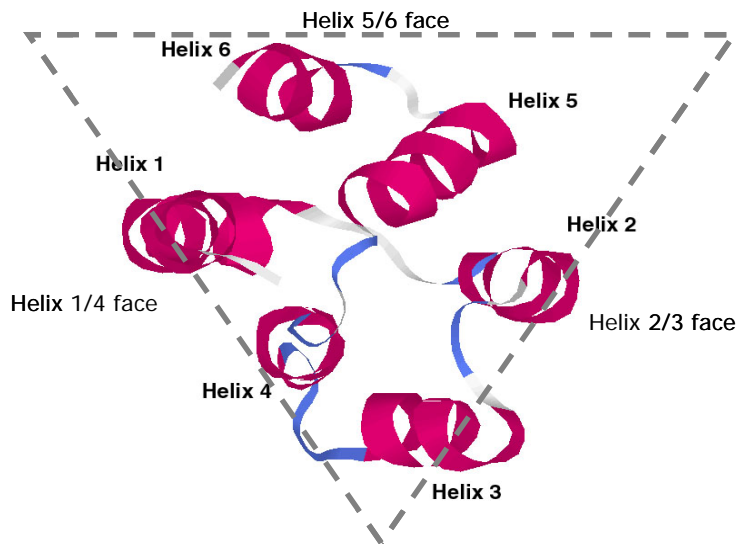
Figure 20. Schematic of the Bcl10 CARD

The six alpha helices of the Bcl10 CARD with the three helical binding faces are represented, as predicted by computer homology modeling. (Lambert et al. 2002. *Bioinformatics 18:1250*)

MALT1 interacts with residues in the helix 5/6 face of the Bcl10 CARD

At this point in our analysis of the MALT1 binding domain of Bcl10, we slightly modified our experimental approach. While we confirmed that Bcl10-ΔMALT1 abrogated POLKADOTS formation and NF-κB activation, we also demonstrated that a previously characterized mutant, Bcl10-G78R, similarly affected POLKADOTS formation and NF-κB activation. Bcl10-G78R is known to destabilize the Bcl10 CARD (39) and it is likely that this structural change led to the phenotype we observed. Hence, it was possible that the phenotype of the Bcl10 point mutants we generated within the Bcl10 CARD might also be accounted for by a critical CARD structural change, rather than a direct effect on MALT1 binding. To discriminate between these two possibilities, we examined the ability of our Bcl10 point mutants to interact directly with MALT1 (by co-immunoprecipitation assay, as we had done previously for the D7-D9 mutants), and we also evaluated their ability to functionally interact with the CARD of CARMA1 (a distinct binding partner of Bcl10).

For this set of mutations, we targeted inter-species conserved amino acid residues that were predicted to be solvent-exposed, based on our threading model of the Bcl10 CARD (*Table 3*). We tried to avoid mutating any residues that might destabilize the CARD structure (i.e., residues that might be involved in intramolecular helix-helix interactions within the CARD). These Bcl10 point mutants were generated as before and included residues from the amino acid region 80 to 104. A previously generated double-point mutant, DE101,102VV, was also included in this analysis, since this mutant included two hydrophilic residues in helix 6. However, it is important to note that, based on our threading model of the Bcl10 CARD, only D101 lies exposed on the helix 5/6 face, while E102 may be involved in a stabilizing interaction with K17 in helix 1 (*data not shown*).

		80		82		84		86		88		90		92		94		96		98		100		102		104
Mouse	L	D	T	L	V	E	S	I	R	R	E	K	T	Q	S	F	L	I	Q	K	I	T	D	E	V	L
Human	L	D	T	L	V	E	S	I	R	R	E	K	T	Q	N	F	L	I	Q	K	I	T	D	E	V	L
Rat	L	D	T	L	V	E	S	I	R	R	E	K	T	Q	N	F	L	I	Q	K	I	T	D	E	V	L
Chicken	L	D	A	L	V	E	S	I	R	R	E	R	T	Q	N	F	L	L	Q	K	I	T	D	I	V	L
Fugu	L	D	A	L	T	D	S	I	R	E	M	R	S	Q	N	F	I	I	T	K	I	T	D	E	V	Q
Consensus	L	D	T/A	L	V/T	E/D	S	I	R	X	X	K/R	T/S	Q	S/N	F	L/I	I	Q/L/T	K	I	T	D	X	V	L/Q
Solvent exposure	*	*		*								*	*	*	*		*	*				*	*			
D80A		A																								
E84A						A																				
R87A									A																	
K90A												A														
Q92A														A												
L95K																	K									
I96K																		K								
Q97A																			A							
K98A																				A						
I99K																					K					
T100A																						A				
DE101,102VV																							V	V		
V103K																									K	

Table 3. Helix 5/6 mutations alignment. The inter-species conserved residues aa80-104 are represented, with the consensus sequence below. An X indicates no consensus at that position. Listed below are each of the Bcl10 point mutants we generated for this region, with the specific amino acid substitution(s) indicated.

Three Bcl10 mutant subsets were represented in this region of mutagenesis: (going from C-terminus to N-terminus) helix 6, the loop that connects helix 6 to helix 5,

and helix 5. We identified five null mutants of Bcl10 (based NF-κB activation) from

helix 6: L95K, I96K, I99K, DE101,102VV, and V103K. We identified one Bcl10 null

mutant from the helix 5/6 loop: Q92A, and we identified two Bcl10 null or highly

impaired mutants from helix 5: D80A and E84A (*Figure 21*).
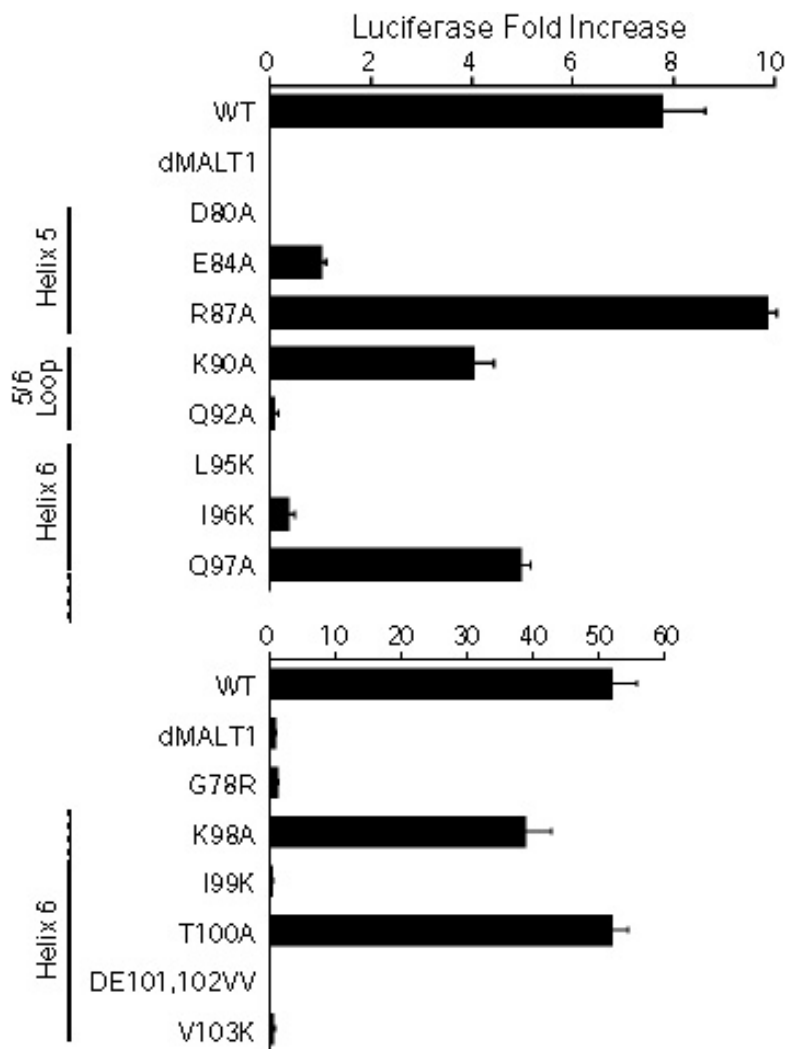
Figure 21. Several residues in the helix 5/6 face of the Bcl10 CARD are required for NF-κB activation

293T cells were transiently transfected with a Bcl10-construct and NF-κB luciferase assay reporter vectors. After 48 hrs, cell lysates were recovered and assayed for NF-κB activation as measured by fold luciferase increase relative to the reporter vector, only and transfection efficiency. Relative to the Bcl10-WT and Bcl10-dMALT1 controls, eight mutants from the helix 5/6 face failed to activate or were highly impaired in activation of NF-κB (D80A, E84A, Q92A, L95K, I96K, I99K, DE101,102VV, and V103K). G78R was used as a negative control in this study. Each Bcl10-construct was assayed in triplicate and error bars represent the standard deviation.

We co-immunoprecipitated FLAG-tagged MALT1 with 3xHA-tagged Bcl10-WT,

-ΔMALT1, several of the null Bcl10 mutants (From helix 5: D80A; From the helix 5/6

loop: Q92A; From helix 6: I96K, DE101,102VV, and V103K; From the minimal

MALT1 binding site: L106K and KKK>AAA) and several of the positive Bcl10 mutants

(From helix 5: R87A; From helix 6: Q97A and T100A; From the minimal MALT1

binding site: R107A, EH112,113AA, and K115A) that we had generated. First, as a

control, we co-immunoprecipitated various MALT1 constructs with Bcl10-WT (*Figures*

22 & 23). To ensure that our co-immunoprecipitation studies were specific for the

interaction between the Ig-like domains of MALT1 and Bcl10, we observed the ability of

Bcl10 to interact with MALT1 Ig-like domain deletion constructs. We observed that, as

expected, Bcl10 can only interact with the Ig-like domains of MALT1.

Figure 22. MALT1 deletion constructs
These constructs were generated as described in Methods. The MALT1-DD-only and MALT1-dN constructs lacked the Ig-like domains required for binding to Bcl10.

Figure 23. Bcl10 interaction with MALT1 is specific for the Ig-like domains
293T cells were co-transfected with 3xHA-tagged Bcl10-WT or -dMALT1 and various FLAG-MALT1 constructs. After 48 hrs, cell lysates were recovered and subjected to 1μg anti-FLAG antibody capture and 20μl Protein G sepharose recovery. Following protein separation by SDS-PAGE, immunoblots were probed with anti-HA antibody. Compared to MALT1-N-only, MALT1-DD-only and MALT1-dN failed to capture Bcl10-WT.

Having co-immunoprecipitated FLAG-tagged MALT1 with the 3xHA-tagged

Bcl10 constructs listed above, we found that, with the exception of the null mutant Q92A,

MALT1 could not capture any of the null Bcl10 mutants. However, MALT1

successfully pulled down Bcl10-WT and the positive Bcl10 mutants (although it

interacted weakly with Bcl10-T100A). Hence, eight point mutations within the CARD

are critical for MALT1 binding and, from these data, we concluded that MALT1 can bind

to helix 5 and helix 6 of the Bcl10 CARD (*Figure 24 & Table 4*). Also, in general, there

is a correlation between NF-κB activation and MALT1 binding. However, for the two

mutants, Q92A and T100A, this correlation was not strong, thus suggesting that other

activities regulated by this region may contribute to NF-κB activation.
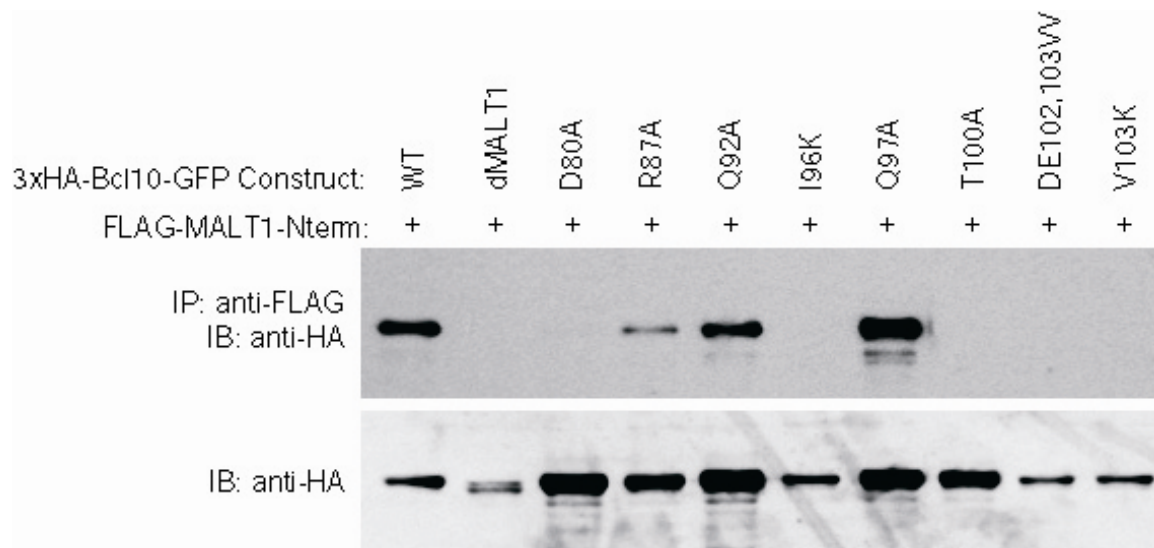
Figure 24. MALT1 interacts with residues from Bcl10 helices 5 & 6
      293T cells were co-transfected with a 3xHA-tagged Bcl10-construct and FLAG-MALT1. After 48 hrs, cell lysates were recovered and subjected to 1μg anti-FLAG antibody capture and 20μl Protein G sepharose recovery. Following protein separation by SDS-PAGE, immunoblots were probed with anti-HA antibody. FLAG-MALT1 successfully captured the positive mutants: Bcl10-WT, -R87A, -Q97A, and -T100A. Although no T100A band is visible in this image, multiple experiments revealed a weak Bcl10-T100A band. FLAG-MALT1 failed to capture the null mutants: Bcl10-dMALT1, -D80A, -I96K, -DE101,102VV, and -V103K. Unexpectedly, FLAG-MALT1 strongly interacted with the null construct, Bcl10-Q92A.

Bcl10-GFP Construct	NF-κB Activation	MALT1 IP	CARMA1 phosphorylation
WT	++++	Y	Y
dMALT1	-	N	N
G78R	-	NE	N
D80A	-	N	Y
E84A	+	NE	NE
R87A	++++	Y	Y
K90A	+++	NE	NE
Q92A	-	Y	Y
L95K	-	NE	NE
I96K	-	N	N
Q97A	++	Y	Y
K98A	+++	NE	NE
I99K	-	NE	NE
T100A	++++	Y(weak)	Y
DE102,103VV	-	N	N
V103K	-	N	N

++++, >75% WT activation
+++, 50% - 75% WT activation
++, 25% - 50% WT activation
+, 10% - 25% WT activation
-, Less than 10% WT activation
Y, yes; N, no; NE, not examined

Table 4. NF-κB activation correlates with MALT1 binding as assessed by co-immunoprecipitation With the exception of mutant Q92A, Bcl10 mutants that failed to activate NF-κB could not be captured by FLAG-MALT1.

Several Bcl10 CARD mutants retain the ability to functionally interact with

CARMA1 and are, therefore, properly folded

Next, we performed experiments to measure the relative ability of the Bcl10 point

mutants to functionally interact with CARMA1. These experiments were performed by

co-transfecting 293T cells with CARMA1 and our various Bcl10 mutants,

immunoblotting the cell lysates, and probing for the presence of phosphorylated Bcl10.

Work from this laboratory previously demonstrated that TCR engagement stimulates the

formation of a more slowly migrating form of Bcl10 as assessed by immunoblot. This

slowly migrating form of Bcl10 is phosphorylated, as demonstrated by λ-phosphatase

treatment (66). The rationale behind these experiments is that, when CARMA1 interacts

with Bcl10, it induces Bcl10 activation and phosphorylation (20). Our results showed

that, relative to Bcl10-G78R (described above), most of our mutations supported efficient

Bcl10 phosphorylation by the CARMA1 co-transfection assay. However, mutants

DE101,102VV and V103K could not be successfully phosphorylated (<5% of WT levels).

In addition, mutants Q92A and I96K appeared somewhat deficient in Bcl10

phosphorylation, although these differences were not statistically significant. Importantly,

D80A, I96K, L106K, and KKK>AAA clearly retained the ability to be efficiently

phosphorylated upon interaction with CARMA1. Therefore, the Bcl10 CARD is properly

folded and our conclusions regarding the extended MALT1 binding site, including the

Bcl10 CARD (helices 5 and 6), appear to be valid (*Figures 25, 26, & Table 4*).
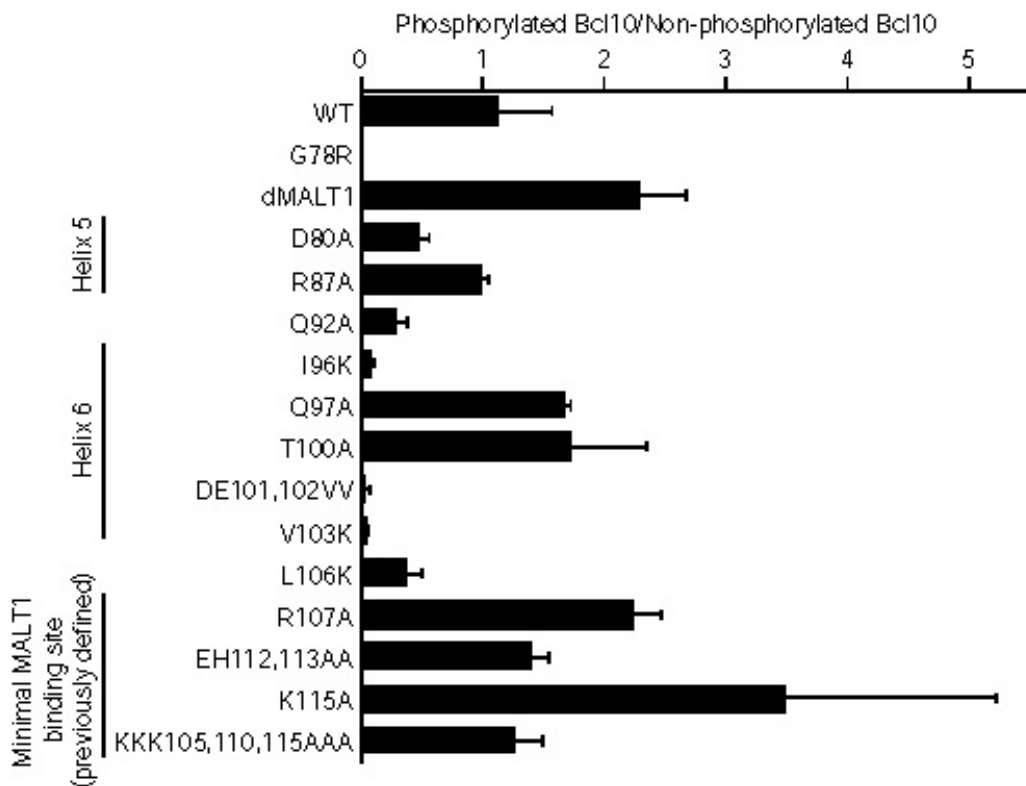
Figure 25. Overall, Bcl10-constructs do not disrupt the Bcl10 CARD
     293T cells were co-transfected with a Bcl10-construct and CARMA1. After 48 hrs, cell lysates were recovered and separated by SDS-PAGE. Immunoblots were probed with anti-Bcl10 antibody and visualized following incubation with an HRP-conjugated secondary antibody. Bcl10 protein bands were imaged with a Fuji LAS-3000 CCD camera system and quantified using MultiGauge 3.0 software (Fuji). The relative intensities of phosphorylated Bcl10 to unphosphorylated Bcl10 were measured in triplicate for each Bcl10-construct. Error bars represent the standard deviation. Relative to the Bcl10-WT positive control, only two mutants (DE101,102VV and V103K) resulted in a significant reduction in CARMA1-mediated phosphorylation of the Bcl10 CARD.

Figure 26. A representative immunoblot from the CARMA1 co-transfection assay
　　　For each Bcl10 construct represented (WT, G78R, dMALT1), the experiment was performed in triplicate. On the immunoblot, the upper band was phosphorylated Bcl10 and the lower band was unphosphorylated Bcl10.
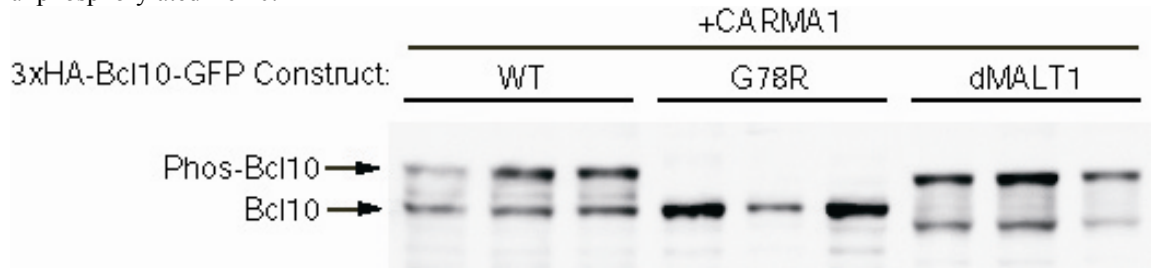
The MALT1 binding domain of Bcl10 extends upstream of aa107 and includes the

helix 5/6 face of the Bcl10 CARD

Taken together our data suggest that the Bcl10 binding domain for MALT1 is not confined to amino acid region 107-119, as previously described, but is minimally defined by the amino acid region 80-114, and is predominantly located within the helix 5/6 face of the Bcl10 CARD. This much larger region might be better expected to accommodate the two Ig-like domains of MALT1 that are known to bind to Bcl10 (46, 84). Additionally, the DEVL region of this domain appears to play a role in stabilizing the Bcl10 CARD.

This binding region also includes a portion of a CARD, which is commonly assumed to allow only homotypic (CARD-CARD) interactions. To date, only one other group has identified a CARD-containing protein, ARC (an apoptosis inhibitor), that can interact with non-CARD proteins through its CARD (51). However, the portion of the CARD used by ARC to bind to non-CARD proteins was not defined in this study. There are over 40 known proteins that contain a CARD (including Bcl10) and the current literature suggests that none of them can engage in heterotypic (CARD-non-CARD) interactions.

The MALT1 binding domain is likely to be distinct from the CARD-CARD binding

domain of Bcl10

The results of the Bcl10-CARMA1 co-transfection assay, also suggested to us that

the 5/6 face of the Bcl10 CARD may not be the site of CARMA1 binding. Because the

majority of the mutants were able to interact with CARMA1 and were robustly

phosphorylated, it is extremely unlikely that CARMA1 binds at this site. This finding is

also consistent with the literature that describes CARD proteins as interacting through

their 1/4 and 2/3 faces (90). Perhaps, the 5/6 face of the Bcl10 CARD only permits

CARD-non-CARD interactions, as suggested by our MALT1 binding data. This raises

the intriguing possibility that Bcl10 can complex with multiple proteins coordinately.

Further point mutations to the helix 1/4 and 2/3 faces of the Bcl10 CARD would be

required to confirm this binding distinction, and this work is ongoing in the lab.

The Bcl10 C-terminus negatively regulates POLKADOTS formation

We were struck by an interesting phenotype of two of our mutants, Bcl10-D7-

GFP and Bcl10-D8-GFP. When we introduced these mutations into D10 T cell clones

and visualized POLKADOTS using microscopy, we recognized that these mutants

robustly formed POLKADOTS even in the absence of T cell activation (i.e. without

antigen stimulation). These spontaneous POLKADOTS continued unabated following

T cell activation, and these mutants could also still activate NF-κB as assessed by

luciferase assay. This led us to consider that the C-terminus of Bcl10 may suppress the

ability of Bcl10 to form POLKADOTS. Since we were unsure how much of the C-

terminus was involved in this suppression, we made several progressive Bcl10 C-terminal

truncations, ultimately encompassing the entire C-terminus. From C-terminus to N-

terminus, we generated Bcl10-D1 (216), -D2 (195), -D3 (175), -D4 (155), -D5 (135), -D6 (122), -D7 (118), -D8 (114), and –D9 (106) (*Figure 27*).
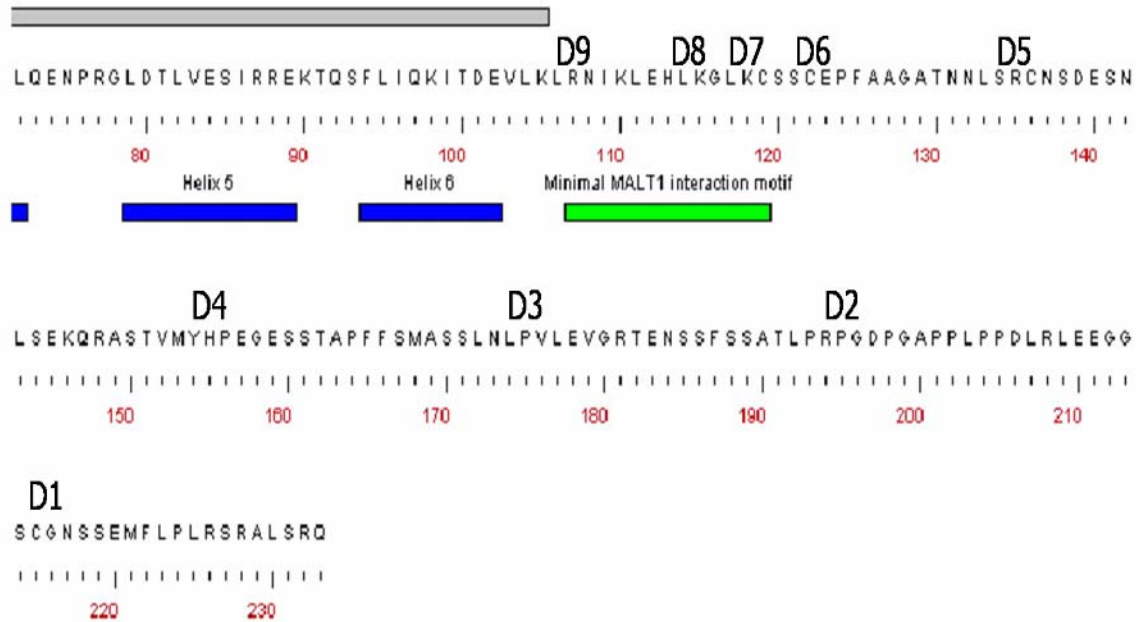
Figure 27. Bcl10 C-terminal deletions
   The deletions 1-9 truncated Bcl10 at the sites indicated.

We examined each of these deletion mutants for the presence of POLKADOTS in activated D10 T cells and found that only Bcl10-D9 failed to form POLKADOTS. We also examined each for spontaneous POLKADOTS formation in inactivated D10 T cells and found that only Bcl10-D7 and Bcl10-D8 formed spontaneous POLKADOTS. Next, we examined all of the deletion mutants for relative NF-κB activation by luciferase assay and found that only Bcl10-D9 entirely failed to activate NF-κB, although Bcl10-D3 varied between substantial impairment to apparent failure to activate NF-κB (*Figure 28*). We are still in the process of determining whether the D7 and D8 mutants show spontaneous NF-κB activation in T cells, which might be expected given their spontaneous POLKADOTS formation phenotype. From these data, we hypothesized that a regulatory region lies between D7 and D6, below which spontaneous POLKADOTS

largely cease to occur. These observations are consistent with previous findings that suggest that Bcl10 may self-oligomerize and thereby induce MALT1 to oligomerize and activate NF-κB (39). The region bounded by D7 (aa118) and D6 (aa122) may normally prevent this oligomerization from occurring spontaneously.
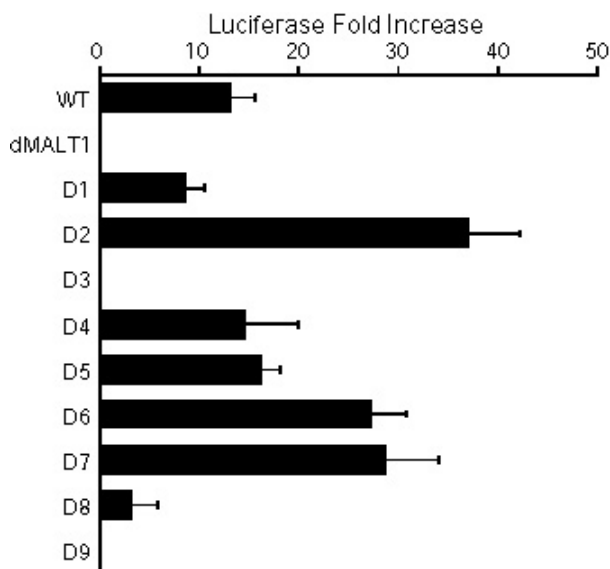
Figure 28. Progressive deletion of the Bcl10 C-terminus reveals two potential regulatory domains

293T cells were transiently transfected with a Bcl10-deletion construct and NF-κB luciferase assay reporter vectors. After 48 hrs, cell lysates were recovered and assayed for NF-κB activation as measured by fold luciferase increase relative to reporter vector, alone and transfection efficiency. Relative to the Bcl10-WT and Bcl10-dMALT1 controls, two mutants (D3 and D9) failed to activate NF-κB: D9=not at all; D3=inconsistent activation. Each Bcl10-construct was assayed in triplicate and error bars represent the standard deviation.

The Bcl10 C-terminus may be the direct target of Bcl10 phosphorylation

A recent study demonstrated that Bcl10 is capable of being phosphorylated at serines 218 and 231 (encompassed by Bcl10-D1) of the Bcl10 C-terminus (96). And in our NF-κB luciferase assay, Bcl10-D3 failed to reliably activate NF-κB. Since Bcl10 phosphorylation is partially correlated with Bcl10 activation, and the significance of Bcl10 phosphorylation is unknown, we decided to examine whether our deletion mutants might effect Bcl10 phosphorylation. We activated Bcl10-D1 to Bcl10-D6 D10 T cell clones in six-well plates on immobilized αTCR antibody for 1 hr, immunoblotted the cell lysates, and probed for phosphorylated Bcl10. We found that Bcl10 phosphorylation, relative to Bcl10-WT, was abolished upstream of Bcl10-D3. Hence, the C-terminus downstream of amino acid 175 is required for Bcl10 phosphorylation. However, even in the absence of this region, Bcl10 could still activate NF-κB (*Table 5*).

Bcl10-GFP Construct	Bcl10 phosphorylation
WT	Y
dMALT1	Y
D1	Y
D2	Y
D3	Y
D4	N
D5	N
D6	N
D7	NE
D8	NE
D9	NE

Y, yes; N, no; NE, not examined

Table 5. The Bcl10 C-terminus is phosphorylated

D10 T cells expressing Bcl10-constructs were stimulated on 100μg/ml plate-bound anti-TCR antibody for 1 hr. Cell lysates were recovered, denatured, and separated by SDS-PAGE. Immunoblots were probed with anti-Bcl10 antibody and visualized following incubation with an HRP-conjugated secondary antibody. Evidence of Bcl10 phosphorylation subsequent to D10 T cell stimulation is observed downstream of aa 175 (D3).

To summarize our findings: MALT1 is capable of binding to the helix 5/6 face of the Bcl10 CARD; other CARD-containing binding partners of Bcl10 are likely to bind to the helix 1/4 and 2/3 faces of the Bcl10 CARD; the Bcl10 C-terminus aa118-122 negatively regulates POLKADOTS formation; and the Bcl10 C-terminus downstream of aa175 regulates and/or contains the specific sites of Bcl10 phosphorylation (*Figure 29*).
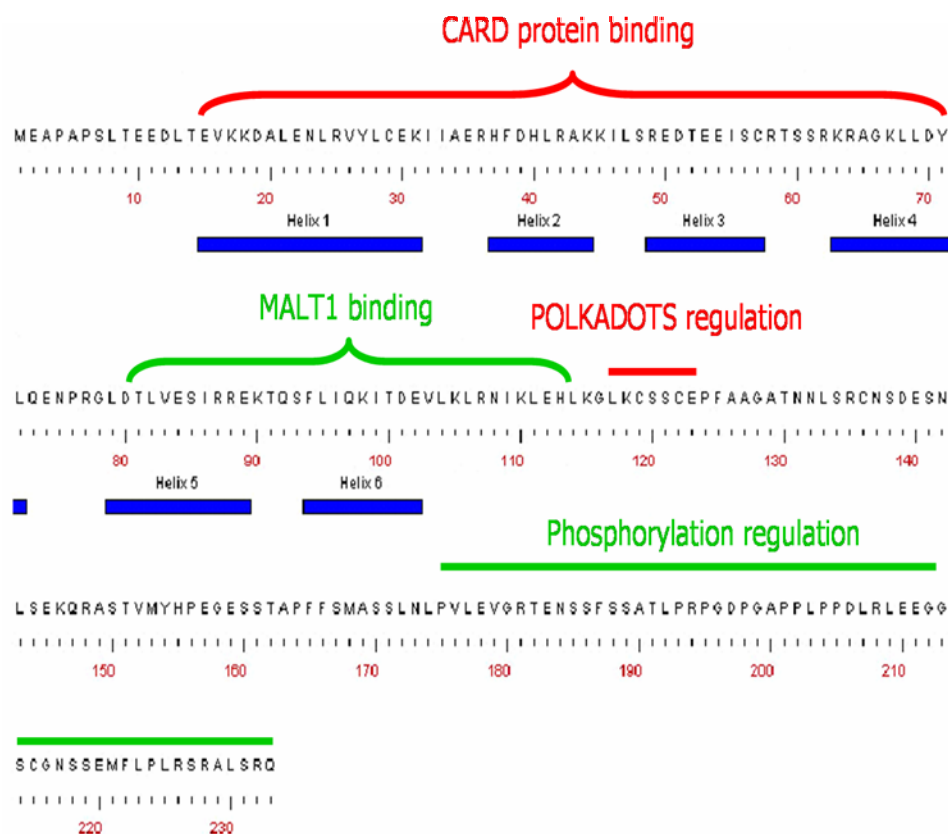
Figure 29. Bcl10 functional domains-revised

This is a representation of the Bcl10 gene and the revised functional domains as suggested by our data.

Chapter 4. Discussion

A critical signal transduction pathway in T lymphocytes that begins with the ligation of the TCR and leads to the activation of NF-κB has only recently begun to be elucidated. While several key signaling intermediates in this pathway have been identified, the details of how they interact with one another to transmit the signal from the activated TCR to NF-κB is largely unknown. Bcl10 is an adaptor protein that is found in a variety of cell types and that is known to play a central role in T cell activation. It directly connects the upstream signaling components of the TCR-to-NF-κB pathway to the downstream signaling components. How Bcl10 propagates the activation signal along the pathway is not known.

Additionally, the crystal structure of Bcl10 has not been solved. Through homology to other proteins, Bcl10 has been described as possessing an N-terminal CARD, but, conversely, it has a C-terminus bearing no similarity to any other protein. Following its activation by an unknown mechanism through PKCθ, Bcl10 is thought to associate with and regulate a key signaling complex comprised of CARMA1 and oligomers of MALT1 and TRAF6 (9, 20, 57, 74). Precisely how Bcl10 interacts with its partner signaling proteins remains speculative, but it is currently believed that Bcl10 binds to partner CARD proteins through its CARD and interacts with MALT1 through a thirteen amino acid region located between the CARD and the C-terminus (5, 6, 20, 46, 47, 56, 59, 94). The purpose of this work has been to characterize the functional domains of Bcl10 in order to elucidate the mechanisms by which Bcl10 functions to regulate the activities of its signaling partners.

We began our study of Bcl10 by deleting the previously described thirteen amino acid (aa107-aa119) MALT1 binding domain (46). We demonstrated that deletion of this domain abrogates Bcl10 interaction with MALT1 as measured by Bcl10's ability to form POLKADOTS and its ability to activate NF-κB by luciferase assay (*Figures 15 & 16*). Next, to identify the specific amino acids responsible for the interaction of Bcl10 with MALT1, we mutagenized conserved residues in the MALT1 binding region. We were surprised to find that no single mutation was critical for binding and, yet, we had identified one mutation (L106K) upstream of the originally defined binding site that critically affected binding (*Table 2; Figure 16*). To confirm these findings, we made progressive C-terminal deletions through the MALT1 binding domain to isolate the amino acids most essential for MALT1 binding to Bcl10. Utilizing microscopy, NF-κB luciferase assay, and co-immunoprecipitation, we identified a region upstream of aa114 that appeared to be essential for MALT1 binding (*Figures 18 & 19*). Once again, the data placed the binding region further upstream than had previously been described. Also, because this newly defined region appeared to be too small to accommodate the two Ig-like domains of MALT1 required for binding to Bcl10, we reasoned that the rest of the binding site must lie further upstream, extending into the Bcl10 CARD.

We began our study of the Bcl10 CARD by creating a 3-D homology-based model of the CARD. We used a computer program (40) to predict a structure for the CARD and to align it with the Bcl10 protein sequence (*Figure 20*). From this model, we identified a 5/6 helical face that could serve as a binding site for MALT1. In addition, this helix 5/6 face was predicted to lie immediately adjacent to the region that we had already defined as being essential for MALT1 binding.

We mutagenized conserved residues of the helix 5/6 face that were also predicted to be solvent-exposed, based on our computer model. Using the NF-κB luciferase assay, we identified eight point mutants essential for MALT1 binding to Bcl10 (*Figure 21*). To confirm these findings, we co-immunoprecipitated several of the mutants (some critical for MALT1 binding and some not) with FLAG-MALT1 (*Figure 24*). We found that, with the exception of one critical mutation (Q92A) that should not have interacted with MALT1, the rest of the mutations behaved as expected (*Table 4*). Hence, mutations that disrupted the MALT1 binding site could no longer interact with MALT1, while mutations that had no effect on the MALT1 binding site continued to interact with MALT1. With these data, we now had several lines of evidence suggesting that MALT1 binds upstream of aa114 and to the helix 5/6 face of the Bcl10 CARD.

We were concerned, however, that the mutations we had generated in the CARD might, in fact, have destabilized the CARD. A misfolded Bcl10 CARD could also account for the inability of mutants to bind to MALT1 and fail to activate NF-κB. Using a co-transfection assay, we examined the mutant CARD for its ability to functionally interact with CARMA1 (a CARD-containing protein) via the induction of Bcl10 phosphorylation. We found that only two of our mutations (DE101,102VV and V103K) resulted in significant impairment of CARMA1-mediated Bcl10 phosphorylation (*Figure 25*). Hence, we reasoned that these two mutants had no direct impact on MALT1 binding and, instead, acted to stabilize the CARD structure. Since the majority of our mutants successfully interacted with CARMA1, the Bcl10 CARD appeared to be functionally intact and our observations regarding MALT1 binding appeared to be valid.

We still had to account for two mutations for which the data was not as we had expected. For mutant Q92A, which could not activate NF-κB, but could strongly interact with MALT1 and for mutant T100A, which could potently activate NF-κB (and could form POLKADOTS), but could only weakly interact with MALT1, there were various possible explanations of the data. One plausible explanation is that there may be an additional binding partner that stabilizes the interaction between Bcl10 and MALT1, which is variably affected by our point mutants. In this case, the T100A mutant would appear to interact poorly with MALT1, because the hypothetical binding partner was not included in the co-transfection. Indeed, CARMA1 is a known binding partner of both Bcl10 and MALT1 (6, 9, 19, 20, 56), and this protein might be expected to play such a role. Alternatively, perhaps there is an activation-induced conformational change of Bcl10, which is variably affected by the point mutants, and which is required for NF-κB activation by the Bcl10-MALT1 complex. In this case, the Q92A mutant might still bind to MALT1 (and CARMA1), but be unable to transduce an activating signal to NF-κB, due to its inability to undergo this hypothetical conformational change. A distinct possibility is that certain mutations (e.g., Q92A) affect the ability of Bcl10 to oligomerize. Since evidence suggests that oligomerization is required for Bcl10-mediated activation of NF-κB (39, 46), a mutation that allows MALT1 and CARMA1 binding to the Bcl10 CARD, but prevents CARD-dependent oligomerization, would be predicted to fail to activate NF-κB. The above and similar hypotheses could explain the unexpected behavior of the Q92A and T100A mutants. Subjecting more of the mutants to co-immunoprecipitation with FLAG-MALT1 would better elucidate precisely how MALT1 interacts with Bcl10 in this region, and these studies are in progress.

In light of our observation that MALT1 (a non-CARD protein) was able to bind to the Bcl10 CARD, and that this binding was physiologically significant, we considered whether CARD-containing proteins could also bind to this region. The results of the CARMA1 co-transfection assay (*Figure 25*), suggested to us that CARMA1 does not bind to the helix 5/6 face. The ability of CARMA1 to strongly interact with the majority of the helix 5/6 mutants, makes it very unlikely that CARMA1 binds to this region. Hence, the helix 5/6 face of the Bcl10 CARD appears to be a site of heterotypic (CARD-non-CARD) protein interactions, rather than a site of homotypic (CARD-CARD) protein interactions. These data led us to reason that, consistent with the literature (90), Bcl10 homotypic (i.e., CARD-CARD) protein interactions likely occur at the helix 1/4 and helix 2/3 faces. This raises the possibility that Bcl10 can coordinately interact with partner proteins heterotypically and homotypically, possibly resulting in the generation of a multimeric protein signaling complex.

Finally, we examined the C-terminus of Bcl10 to elucidate a function for this uncharacterized region. As we were studying the deletion mutants for their ability to bind to MALT1, we noticed that two of the mutants (D7 and D8) were able to form POLKADOTS in the absence of T cell activation. Since deleting the C-terminus allowed POLKADOTS to form spontaneously, we hypothesized that the C-terminus may negatively regulate POLKADOTS formation. To address this hypothesis, we made progressive C-terminal truncations of Bcl10, starting with amino acids farthest downstream and ending with aa106 (D9), and examined them for POLKADOTS formation and NF-κB activation by luciferase assay (*Figure 28*). We determined that spontaneous POLKADOTS cease to occur downstream of D6 (aa122) and that NF-κB

activation is somewhat impaired downstream of D6. From these data, we reasoned that a regulatory element lies in the region between D6 and D7 (aa118) that prevents spontaneous POLKADOTS formation, perhaps through a conformational change associated with Bcl10 oligomerization, and that may also modulate NF-κB activation.

We further evaluated a potential regulatory role for the C-terminus by examining the D1-D6 truncations for their ability to be phosphorylated (*Table 5*). Bcl10 phosphorylation is partially correlated with Bcl10 activation and we now had data suggesting that the C-terminus may modulate NF-κB activation. Subsequently, we identified a site downstream of aa175 that affects both NF-κB activation and Bcl10 phosphorylation, and may serve as a second regulatory site.

We have hypothesized that phosphorylation of the C-terminus may contribute to, but is not absolutely required for, a conformational change that unmasks a region of Bcl10 that is required for NF-κB activation (e.g., the C-terminus physically masks part of the Bcl10 CARD, until the C-terminus is phosphorylated, thereby triggering a conformational change that unmasks the CARD). When the region containing the phosphorylation domain is deleted, the conformational change, and consequent NF-kB activation, is much less efficient. However, when the majority of the C-terminus is deleted, the masking domain is no longer present, so Bcl10 can again be fully activated, even in the absence of phosphorylation.

Taken together, our data has allowed us to: (1) identify a novel binding site for MALT1 in the Bcl10 protein; (2) suggest that this binding site is distinct from the binding sites of other (CARD-containing) Bcl10 binding partners; and (3) propose two potential regulatory functions for the C-terminus of Bcl10. These results highlight the complex

biology of Bcl10 and serve to broaden the scope of investigation necessary to fully

understand the molecular mechanisms that facilitate signal transduction by this critical

protein intermediate in the TCR-to-NF-κB pathway.

Chapter 5. Experimental Methods

Methods (Aim 1)

Cell lines and tissue culture

The murine T cell clone, D10-IL2, was utilized for these experiments. D10-IL2 is an IL-2-dependent subclone of the CD4$^+$ T cell clone D10 G4 (37). It is maintained in Click's (EHAA) media supplemented with 10% fetal bovine serum and the cytokine, IL-2. In experiments requiring APCs, the CH12 H-2^k-positive B cell line (35), derived from a murine B cell lymphoma, was used and maintained in Click's without added cytokine. For transient transfections, HEK-293T (293T; human embryonic kidney) cells were utilized and maintained in DMEM media supplemented with heat-inactivated 10% fetal bovine serum and 1% Penicillin G/Streptomycin sulfate/Gentamycin sulfate/Glutamine (PSGG) supplement.

Antibodies and reagents

Conalbumin protein was purchased from Sigma. Bcl10 was detected with a rabbit polyclonal primary antibody (H-197) (Santa Cruz Biotech), followed by an HRP-conjugated anti-rabbit secondary antibody (Jackson ImmunoResearch). Bcl10 constructs fused to the 3xHA epitope tag were similarly detected with a rabbit polyclonal anti-HA-tag antibody (Y-11) (Santa Cruz Biotech). In immunoprecipitation experiments, FLAG epitope-tagged MALT1 was captured with a mouse monoclonal anti-FLAG antibody (M2) (Sigma) followed by Protein G sepharose (Pharmacia).

Generation of plasmids

The cDNAs encoding murine Bcl10 and MALT1 were obtained from IMAGE consortium expressed sequence tag (EST) clones (Invitrogen and ATCC). The CARMA1

cDNA was a gift from J. Pomerantz (Johns Hopkins University) and D. Baltimore

(Caltech). Green fluorescent protein (GFP) was fused to the C-terminus of MSCV-

Bcl10-wild-type (WT) in a modified method as described by Schaefer, *et al* (66) (*Figure*

30). FLAG-MALT1-ΔC (pcDNA3-F-MALT1-YCit A/K) was generated by

HindIII/NotI digestion of F-MALT1-YCit-A/K with insertion into pcDNA (Invitrogen).

MSCV-Bcl10-GFP-ΔMALT1 was generated by PCR amplification of Bcl10 using sense

primer (Δaa107-119) 5'-GAAAAGCTTAGCAGCTGTGAGCCCTTT-3' and anti-sense

primer (#2438) 5'-GATACGCGTCCTTGGCGTGAAAGAGCCCGTGACCGTAA-3'.

The resulting fragment was digested with HindIII/MluI. MSCV-Bcl10-GFP was digested

in two parts with NcoI/MluI and NcoI/HindIII. The PCR fragment and the two MSCV

fragments were 3-part ligated at the HindIII/MluI site. MSCV-Bcl10-GFP-

DE101,102VV was generated by PCR amplification of Bcl10 using sense primer (#2437)

5'-GGGCCATGGAGGCTCCCGCACCGTCCCTCA-3' and anti-sense primer 5'-

GAAAAGCTTTAGCAC<u>CACAAC</u>CGTTATCTTCTGAATC-3'. The resulting

fragment was digested with NcoI/HindIII. MSCV-Bcl10-GFP was digested in two parts

with NcoI/MluI and MluI/HindIII. The PCR fragment and the two MSCV fragments

were 3-part ligated at the NcoI/HindIII site. MSCV-Bcl10-GFP-L95K, –I96K, –Q97A, -

K98A, -I99K, -T100A, and -V103K were generated by PCR amplification using sense

primer #2437 and a sequence-specific anti-sense primer. The PCR fragment was

digested with NcoI/HindIII and ligated into MSCV-Bcl10-<u>EcoRI/NotI linker</u>-GFP to

obliterate the redundant HindIII site in the plasmid. MSCV-Bcl10-GFP-K105A, -L106K,

-R107A, -N108A, -K110A, -L111K, -EH112,113AA, -L114K, -K115A, -KKK>AAA,

and –LLL>KKK were generated by PCR amplification using sense primer #2437 and a

sequence-specific anti-sense primer. The PCR fragment was digested with NcoI/StuI and ligated into MSCV-Bcl10-GFP at that site.   MSCV-Bcl10-GFP-deletion 7 (D7) and – deletion 8 (D8) were generated by PCR amplification using sense primer #2437 and a Bcl10 truncated oligomer (D7=aa119, D8=aa115) anti-sense primer.   The PCR fragment was digested with NcoI/MluI and ligated into MSCV-Bcl10-GFP at that site.   MSCV-Bcl10-GFP-deletion 9 (D9=aa107) was generated by digestion of pQE30-Bcl10-CARD-GFP with NcoI/NotI and insertion into MSCV-Bcl10-GFP. MSCV-3xHA-Bcl10-GFP-WT, -ΔMALT1, -DE101,102VV, -I96K, -Q97A, -T100A, -V103K, -L106K, -R107A, -EH112,113AA, -K115A, and –KKK>AAA were generated by digestion of pENeo-3xHA-TSG101-YCit with BglII/NcoI and insertion of the sequence encoding Met-3xHA into the previously generated MSCV Bcl10 mutant to position the 3xHA tag directly upstream of the starting methionine of each mutant cDNA. The pENeo-3xHA-Bcl10-GFP-D7, -D8, and –D9 were generated by digestion of MSCV-3xHA-Bcl10-GFP-WT with NcoI/NotI and insertion of the sequence encoding Met-3xHA into the previously generated pENeo Bcl10 mutant to position the 3xHA tag directly upstream of the starting methionine of each mutant cDNA. All PCR-amplified mutations were sequence verified.

Figure 30. MSCV-Bcl10-
GFP cloning vector

Retroviral construction and infection

For infection of D10 T cells, all MSCV Bcl10 mutant constructs were subcloned

into the MMLV retroviral vector, pENeo (67), at the BglII-NotI restriction site *(Figure*

31). The replication defective pENeo vector was calcium-phosphate transfected (32) into

HEK-293T cells with an ecotropic packaging plasmid (pCL-Eco) to enable virus

production as follows. Six-well plates were coated with poly-D-lysine (100µg/ml in H_2O)

to promote adherence of the 293T cells. The wells were washed six times with 1xPBS

just prior to plating the cells at a density of $6x10^5$cells/well in 1ml of DMEM. Plates

were cultured overnight at $37^oC/5\%CO_2$. At the time of transfection, the growth medium

was replaced with 1.5ml of warmed (37^oC) Iscove's modified Dulbecco's medium

(IMDM, Gibco/BRL), and the calcium phosphate precipitates of plasmid DNA were

added. The precipitates were made by preparing a mixture of 2.4µg of retroviral plasmid DNA, 0.6µg of pCL-Eco helper plasmid, 7.5µl of 2.5M $CaCl_2$, and sterile H_2O to a final volume of 75µl. To this mixture, 75µl of 2x Hepes (140mM NaCl, 1.5mM $NaPO_4$, 50mM Hepes, pH 7.05) solution was added. After exactly 1min, the mixture was dripped onto the cells. The cells were incubated with the DNA precipitates at $37^{\circ}C/5\%CO_2$ for 24hr and then the medium was replaced with 2ml DMEM. The transfected cells were then incubated at $37^{\circ}C/5\%CO_2$ for another 20-24hr and the retrovirus-containing supernatant was harvested into 15ml sterile conicals and stored at $4^{\circ}C$ until used for infections.

The infection (spinfection) protocol used for D10 T cells was as follows. In a sterile 15ml conical, 1×10^6 D10 T cells were spun down at 500 rcf x 5min in 1ml of IL-2-supplemented Click's media. The supernatant was aspirated and replaced with 2ml of viral supernatant. The mixture was ejected into a well of a 24-well plate and 2µl of polybrene was added. The plate was centrifuged at 1200 rcf for 2hr, after which the cells were resuspended and placed in a sterile 15ml conical. The conical was spun at 500 rcf x 5min, the supernatant was aspirated, and the cells were resuspended into a 25ml flask containing 7ml of IL-2-supplemented Click's media. After culturing the cells at $37^{\circ}C/5\%CO_2$ for 48hr, 1µg/ml of G418 antibiotic was added. Survival of successfully infected cells was confirmed after five days of positive selection.

Figure 31. pENeo retroviral vector

FACS analysis

Mutant D10 T cells were screened by FACS within 7-14 days of retroviral

infection. Cells were concentrated to 1×10^{6}/ml by centrifugation and resuspended in

400µl FACS buffer (1x PBS, 2% FBS, 0.1% NaN$_3$ in H$_2$O). Using a FITC filter (also

capable of detecting GFP), wild-type (no GFP) D10 T cells were gated on auto-

fluorescence and designated as the first decade on a FACS-generated histogram.

Subsequent samples of mutant D10 T cells were run against the WT control and any

fluorescence that appeared above the first decade was considered positive for GFP

expression.

T cell/APC conjugation and microscopy

The night before the conjugation experiment, one flask of APCs was pulsed with 25µl of 10mg/ml conalbumin protein/1ml of Click's medium and cultured at 37°C. The next day, $2x10^5$ retrovirally-infected mutant D10 T cells and $2x10^5$ APCs with or without conalbumin were suspended in 100µl each of Click's media. Poly-D-lysine coated cover slips were placed in 35ml dishes, one for each condition, and rinsed with ddH$_2$O. For each condition, 100µl D10 T cells were added to 100µl APCs in an eppendorf tube and centrifuged for 30sec in a picofuge, to facilitate synchronous T cell/APC interactions. The cell mixture was then placed in a 37°C water bath for 10min, gently mixed with a pipettor, and ejected onto one of the poly-D-lysine cover slips. The cell-laden cover slip was incubated at 37°C/5%CO$_2$ for 5min and then fixed with 2ml of cell fix solution (3% paraformaldehyde, 3% sucrose, 1xPBS, pH 7.5) for 10min. The fixative was aspirated and the cover slip was gently washed twice with 1xPBS/0.1% NaN$_3$. The cover slip was mounted in glycerol (90):PBS (10) (note that p-phenylenediamine was also added to reduce photobleaching) onto a glass slide, gently blotted dry, and sealed with clear acrylic nail polish. Three-dimensional (3-D) fluorescent images were taken at room temperature on a Zeiss Axiovert 200M inverted wide-field epifluorescent microscope with a digital charged coupled device (CCD) camera. Computational image restoration was used to obtain 3-D cellular images (68). A xenon lamp with a 488nm excitation filter was used to visualize Bcl10-GFP, and images were digitally deconvolved and projection images generated using a maximal projection algorithm (TILLvisION from TILL Photonics). Utilizing this software package, three-dimensional image stacks were processed into two-dimensional projection images. Images were examined for the

presence of Bcl10 POLKADOTS formation and at least 20 cells were analyzed for each treatment condition.

<div align="center">SDS-PAGE immunoblotting</div>

For Western blotting, a 10% Tris-glycine SDS-Polyacrylamide resolving gel (30% acrylamide mix, 1.0M Tris (pH 8.8), 10% SDS, 30% ammonium persulfate, TEMED, H_2O) was poured into a vertical SDS-PAGE gel apparatus and allowed to polymerize. A 5% Tris-glycine SDS-Polyacrylamide stacking gel (30% acrylamide mix, 1.0M Tris (pH 6.8), 10% SDS, 30% ammonium persulfate, TEMED, H_2O) was poured on top of the resolving gel and allowed to polymerize around a 15-lane comb. Samples in 2x SDS-PAGE loading buffer (1000μl ddH_2O, 880μl SDS, 120μl 2-mercaptoethanol) were prepared with boiling for 4min before loading. 10μl of a protein marker was run in the first lane and 20μl of protein sample was loaded into each of the remaining lanes. The gel was run at 150-250 volts in Tris-glycine buffer for approximately 3hr, after which the apparatus was shut down and the gel removed. The gel was cut down to the appropriate size and gently washed in transfer buffer (0.04% SDS, 20% methanol, 48mM Tris, 39M glycine, H_2O) for 15-20min. Also, six sheets of absorbent paper and one sheet of nitrocellulose were cut to the same dimensions as the gel and gently washed in transfer buffer for 15-20min. The transfer apparatus had a bottom plate anode, such that three sheets of soaked absorbent paper were placed directly on the bottom plate, one soaked nitrocellulose membrane was placed on top of that, one soaked gel was placed on top of that, three sheets of soaked absorbent paper were placed on top of that, and the cathode plate was the last to be placed on top. The transfer apparatus was run in milliamps equivalent to the surface area of the gel (e.g., 100mA for 100cm^2) for 1.5-2hr. The

transfer apparatus was disassembled, the nitrocellulose membrane was removed, and the

membrane was placed in blocking solution (98ml ddH$_2$O, 2ml Tris (pH 7.5), 5g

dehydrated milk) at 4°C with rocking overnight.

Nitrocellulose membranes were probed for Bcl10 with a rabbit polyclonal primary

antibody (H-197) (Santa Cruz Biotech) in blocking solution/0.1% Tween at a 1:1000

concentration for 3hr, followed by an HRP-conjugated anti-rabbit secondary antibody

(Jackson ImmunoResearch) in blocking solution/0.1% Tween at a 1:100,000

concentration for 2hr. Nitrocellulose membranes were probed for 3xHA-Bcl10-GFP with

a rabbit polyclonal anti-HA-tag antibody (Y-11) (Santa Cruz Biotech) in blocking

solution/0.1% Tween at a 1:1000 concentration for 3hr, followed by an HRP-conjugated

anti-rabbit secondary antibody (Jackson ImmunoResearch) in blocking solution/0.1%

Tween at a 1:100,000 concentration for 2hr. Membranes were developed with

SuperSignal West Dura (Pierce), imaged with a Fuji LAS-3000 CCD camera system, and

quantified using MultiGauge 3.0 software (Fuji).

For the Bcl10-CARMA1 co-transfection assay, 6x10^5 293T cells/well were plated

as described for the calcium phosphate protocol. Using a slight variation of this protocol,

1000ng mutant Bcl10-GFP (MSCV-Bcl10-GFP) plasmid DNA, 1000ng CARMA1

(pENeo-Myc-CARMA1) plasmid DNA, 1000ng pBlueScript plasmid DNA (used to

adjust the final plasmid DNA concentration to an equal amount), 7.5µl of 2.5M CaCl$_2$,

and sterile H$_2$O to a final volume of 75µl were mixed. To this mixture, 75µl of 2x Hepes

solution was added and the mix was dripped onto the 293T cells exactly 1min later.

After 48hr of incubation, the cells were washed once in 1ml 1x PBS and lysed in 2x SDS-

PAGE loading buffer with sonication. Approximately 5x10^4 cell equivalents were

separated per lane on a 10% SDS-PAGE gel. The protein was transferred to

nitrocellulose and blocked, as described above, and the membrane was probed for Bcl10.

This experiment was performed in triplicate for each condition.

Co-immunoprecipitation

For the co-immunoprecipitation experiments, $6x10^5$ 293T cells/well were plated as

described for the calcium phosphate protocol. Using a slight variation of this protocol,

1000ng 3xHA-tagged mutant Bcl10-GFP plasmid DNA, 1000ng FLAG-tagged MALT1-

ΔC, 1000ng pBlueScript plasmid DNA, 7.5µl of 2.5M $CaCl_2$, and sterile H_2O to a final

volume of 75µl were mixed. To this mixture, 75µl of 2x Hepes solution was added and

the mix was dripped onto the 293T cells exactly 1min later. After 48hr of incubation, the

cells were washed once in 1ml 1x PBS and incubated in 800µl IP lysis buffer (20mM

Tris pH 7.5, 1% NP40, 0.5% Deoxycholate, 0.25M NaCl, 3mM EDTA, 3mM EGTA)

supplemented (immediately prior to lysis) with a protease inhibitor cocktail (50mM NaF,

1mM Na_3VO_4, 50µM leupeptin, 2µg/ml aprotinin, 1mM DTT, 1mM PMSF) for 30min

on ice. Cells were lysed by pipetting, placed in eppendorf tubes on ice, and centrifuged

at 4^oC at maximum rpm for 10min. Supernatants were carefully (so as not to disturb the

pelleted debris) removed to fresh tubes, to which 20µl of Protein G sepharose was added.

Supernatants were pre-cleared with sepharose at 4^oC with rotation for 1hr. Supernatants

were centrifuged at maximum rpm for 30sec, removed from the sepharose pellet to fresh

tubes, and incubated with 1µg mouse monoclonal anti-FLAG antibody (M2) (Sigma) at

4^oC with rotation for 3hr. 20µl of sepharose was added to the supernatants and

incubation continued for another 1 hr. The sepharose in solution was centrifuged at

maximum rpm for 30sec and the supernatant was discarded. The sepharose pellet was

washed 3 times in 1ml IP lysis buffer, with approximately 30µl of IP lysis buffer left in the tube after the final wash. To this, 30µl of 2x SDS-PAGE loading buffer was added and the pellet was boiled at 100°C for 10min. Immunoprecipitated proteins from approximately $4x10^5$ cell equivalents per condition were separated per lane on a 10% SDS-PAGE gel. The protein was transferred to nitrocellulose and blocked, as described above, and the membrane was probed for 3xHA. This experiment was performed in triplicate for each condition.

NF-κB luciferase assay

For these experiments, $1.2x10^5$ 293T cells were plated per well in a 24-well plate as described for the calcium phosphate protocol. Using a slight variation of this protocol, 112.5ng mutant Bcl10-GFP construct, 4.5ng pBVI-NF-κB-Luc (a luciferase reporter plasmid containing a minimal promoter with multiple NF-κB binding sites; gift from Gabriel Nunez), 49.5ng pEF1-Bos-βgal (a β-galactosidase reporter plasmid; gift from Gabriel Nunez), 45ng pcDNA-p35 (a plasmid used to promote survival of transfected 293T cells; p35 is a baculovirus-encoded homolog of Bcl2, with potent pro-survival activity), and enough pBlueScript (a plasmid used to adjust the final plasmid DNA concentration to an equal amount) for a plasmid DNA total of 600ng were added to a mixture of 4.5µl of 2.5M $CaCl_2$ and sterile H_2O to a final volume of 40.5µl. To this mixture, 45µl of 2x Hepes solution was added and, after exactly 1min, 30µl of the mix was dripped into each of three wells of cells. After 48hrs, the cells were washed once in 300µl 1x PBS, incubated at room temperature in 40µl 1x Reporter Lysis Buffer (Promega) for 15min, and lysed on ice by pipetting. Cell lysates were vortexed and centrifuged at 4°C at maximum rpm for 2min, and supernatants were transferred and divided between a

luciferase plate (20µl for luciferase assay) and a 96-well plate (5µl for β-galactosidase assay). Luciferase Reagent (Promega), containing luciferin, was automatically added by the luminometer to each sample in the luciferase plate. The expressed luciferase in each sample reacted with and cleaved the luciferin, generating light which was measured by the luminometer. The amount of luminescence generated, equated to the amount of luciferase expressed, and this was dependent upon how much NF-κB was bound to the luciferase reporter plasmid promoter. Assay 2x Buffer (Promega) was added to each sample in the 96-well plate, resulting in the development and color change of the expressed β-galactosidase in the cells. After full development had been achieved, 1M sodium carbonate was added to the samples to stop the reaction and the samples were read at the 420nm absorbance wavelength of β-galactosidase on a plate reader. The more intense the color change, the more β-galactosidase was being expressed in each sample, and this equated to the efficiency of transfection (thereby serving as an internal control for each sample).

Methods (Aim 2)

Cell lines and tissue culture

The D10 T cell line and the HEK-293T cell line were used as described in Aim 1. The CH12 B cell line was not used in this Aim.

Antibodies and reagents

As described in Aim 1, Bcl10 was detected with a rabbit polyclonal primary antibody (H-197) (Santa Cruz Biotech), 3xHA-Bcl10 was detected with a rabbit polyclonal anti-HA-tag antibody (Y-11) (Santa Cruz Biotech), and FLAG-tagged proteins

were captured with a mouse monoclonal anti-FLAG antibody (M2) (Sigma) followed by

Protein G sepharose (Pharmacia).

Generation of plasmids

The cDNAs encoding CARMA1 and murine Bcl10 and MALT1 were obtained as

described in Aim 1. MSCV-Bcl10-GFP-WT, MSCV-Bcl10-GFP-ΔMALT1, MSCV-

Bcl10-GFP-DE101,102VV, MSCV-Bcl10-GFP-L95K, –I96K, –Q97A, -K98A, -I99K, -

T100A, MSCV-3xHA-Bcl10-GFP-WT, -ΔMALT1, -DE101,102VV, -I96K, -Q97A, -

T100A, and FLAG-MALT1-ΔC were generated as described in Aim1. MSCV-Bcl10-

GFP-G78R was generated by subcloning the NcoI/NotI fragment from a previously

described plasmid (66). MSCV-Bcl10-GFP-D80A, -E84A, -R87A, and –K90A were

generated by PCR amplification using a sequence-specific sense primer and anti-sense

primer #2438. The PCR fragment was digested with MluI/BstXI and ligated into a non-

methylated MSCV-Bcl10-EcoRI/NotI linker-GFP at that site. This non-methylated

vector plasmid was generated by transforming 1μl of the methylated plasmid (MSCV-

Bcl10-EcoRI/NotI linker-GFP) with 20μl transformation buffer (10mM Hepes (pH 7.7),

50mM CaCl$_2$, 10% glycerol) into Dam-mutant TOP10F' bacteria. Plasmid DNA was

replicated in the bacteria and subsequently purified for use. MSCV-Bcl10-GFP-Q92A

was generated by PCR amplification using sense primer #2437 and a sequence-specific

anti-sense primer. The PCR fragment was digested with NcoI-HindIII and ligated into

MSCV-Bcl10-EcoRI/NotI linker-GFP to obliterate the redundant HindIII site in the

plasmid. MSCV-3xHA-Bcl10-GFP-G78R, -D80A, -R87A, and –Q92A were generated

by digestion of pENeo-3xHA-TSG101-YCit with BglII/NcoI and insertion of the

sequence encoding Met-3xHA into the previously generated MSCV Bcl10 mutant to

position the 3xHA tag directly upstream of the starting methionine of each mutant cDNA.

FLAG-MALT1-ΔN (aa345-832) and FLAG-MALT1-DD-only (aa2-131) were generated

by subcloning a HindIII/NotI fragment encoding the respective construct into the

HindIII/NotI sites of pcDNA3. All PCR-amplified mutations were sequence verified.

SDS-PAGE immunoblotting

Western blotting was performed as described in Aim 1. Bcl10-CARMA1 co-

transfection assay was performed as described in Aim 1.

Co-immunoprecipitation

Co-immunoprecipitation of 3xHA-tagged mutant Bcl10-GFP with FLAG-

MALT1-ΔC was performed as described in Aim 1.

NF-κB luciferase assay

These experiments were performed as described in Aim 1.

Computer modeling of the Bcl10 CARD

ESyPred3D Web Server 1.0 is an automated homology program that employs four

principles of homology modeling to predict a three-dimensional protein structure. The

program searches databanks to identify a structural homolog (template), performs a

target-template alignment, executes model building and optimization, and completes a

model evaluation. The critical step in this four-principled approach is the target-template

alignment, with the strength of the ESyPred3D program being its ability to match the two

homologous segments by incorporating the results of several multiple alignment

programs (40). The template used for this study was the solved crystal structure of

procaspase-9 (accession number 3GYS).

Methods (Aim 3)

Cell lines and tissue culture

The D10 T cell line, CH12 B cell line, and HEK-293T cell line were used as described in Aim 1.

Antibodies and reagents

As described in Aim 1, Bcl10 was detected with a rabbit polyclonal primary antibody (H-197) (Santa Cruz Biotech). For the Bcl10 phosphorylation assays, D10 T cells were stimulated with 100μg/ml plate-bound anti-TCRβ antibody.

Generation of plasmids

The cDNAs encoding murine Bcl10 and MALT1 were obtained as described in Aim 1. MSCV-Bcl10-GFP-WT, MSCV-Bcl10-GFP-ΔMALT1, MSCV-Bcl10-GFP-D7, -D8, and – D9 were generated as described in Aim 1. MSCV-Bcl10-GFP-deletion 1 (D1), –deletion 2 (D2), -deletion 3 (D3), -deletion 4 (D4), -deletion 5 (D5), and -deletion 6 (D6) were generated by PCR amplification using sense primer #2437 and a Bcl10 truncated oligomer (D1=aa216, D2=aa195, D3=aa175, D4=aa155, D5=aa135, D6=aa122) anti-sense primer.   The PCR fragment was digested with NcoI/MluI and ligated into MSCV-Bcl10-GFP at that site. All PCR-amplified mutations were sequence verified.

Retroviral construction and infection

For infection of D10 T cells, all MSCV Bcl10 mutant constructs were subcloned into the MMLV retroviral vector, pENeo (67), at the BglII/NotI restriction site. The method for D10 T cell infection was as described in Aim 1.

FACS analysis

Mutant D10 T cells were screened by FACS as described in Aim 1.

T cell/APC conjugation and microscopy

Molecular imaging of mutant D10 T cells was performed as described in Aim 1.

SDS-PAGE immunoblotting

Western blotting was performed as described in Aim 1. The Bcl10-CARMA1 co-transfection assay was not performed in this Aim.

For the Bcl10 phosphorylation experiments, half of the wells of six-well plates were coated with 1ml αTCR antibody and allowed to incubate at 4°C overnight. The day of the experiment, the αTCR antibody was recovered and the wells were washed six times with 2ml Hanks 1x salt solution. peNeo-Bcl10-GFP-WT, ΔMALT1, -D1, -D2, -D3, -D4, -D5, and -D6 retrovirally-infected mutant D10 T cells were each plated in a well at a density of $2x10^{6}$ cells/1ml IL-2 supplemented Click's media and incubated at 37°C/5%CO_2 for 1 hr. Cells incubated in uncoated wells were designated as time=zero, while cells incubated in αTCR-coated wells were designated as time=60. After incubation, cells were harvested on ice by pipetting into eppendorf tubes. The tubes were centrifuged at 4°C at 1800 rpm x 5min and the supernatant was aspirated. The pelleted cells were resuspended in 150ul 1x SDS-PAGE loading buffer, sonicated for 1min, and boiled at 100°C for 4min. Approximately $2.5x10^{5}$ cell equivalents were separated per lane on an 8% SDS-PAGE gel. The protein was transferred to nitrocellulose and blocked, as described in Aim 1, and the membrane was probed for Bcl10. This experiment was performed in triplicate for each condition.

NF-κB luciferase assay

These experiments were performed as described in Aim 1.

Bibliography

1. **Acuto, O., S. Mise-Omata, G. Mangino, and F. Michel.** 2003. Molecular modifiers of T cell antigen receptor triggering threshold: the mechanism of CD28 costimulatory receptor. Immunol Rev **192:**21-31.

2. **Akagi, T., M. Motegi, A. Tamura, R. Suzuki, Y. Hosokawa, H. Suzuki, H. Ota, S. Nakamura, Y. Morishima, M. Taniwaki, and M. Seto.** 1999. A novel gene, MALT1 at 18q21, is involved in t(11;18) (q21;q21) found in low-grade B-cell lymphoma of mucosa-associated lymphoid tissue. Oncogene **18:**5785-94.

3. **Alessi, D. R., and P. Cohen.** 1998. Mechanism of activation and function of protein kinase B. Curr Opin Genet Dev **8:**55-62.

4. **Berridge, M. J., M. D. Bootman, and P. Lipp.** 1998. Calcium--a life and death signal. Nature **395:**645-8.

5. **Bertin, J., Y. Guo, L. Wang, S. M. Srinivasula, M. D. Jacobson, J. L. Poyet, S. Merriam, M. Q. Du, M. J. Dyer, K. E. Robison, P. S. DiStefano, and E. S. Alnemri.** 2000. CARD9 is a novel caspase recruitment domain-containing protein that interacts with BCL10/CLAP and activates NF-kappa B. J Biol Chem **275:**41082-6.

6. **Bertin, J., L. Wang, Y. Guo, M. D. Jacobson, J. L. Poyet, S. M. Srinivasula, S. Merriam, P. S. DiStefano, and E. S. Alnemri.** 2001. CARD11 and CARD14 are novel caspase recruitment domain (CARD)/membrane-associated guanylate kinase (MAGUK) family members that interact with BCL10 and activate NF-kappa B. J Biol Chem **276:**11877-82.

7. **Beyers, A. D., C. Hanekom, A. Rheeder, A. F. Strachan, M. W. Wooten, and A. E. Nel.** 1988. Characterization of protein kinase C and its isoforms in human T lymphocytes. J Immunol **141:**3463-70.

8. **Bi, K., Y. Tanaka, N. Coudronniere, K. Sugie, S. Hong, M. J. van Stipdonk, and A. Altman.** 2001. Antigen-induced translocation of PKC-theta to membrane rafts is required for T cell activation. Nat Immunol **2:**556-63.

9. **Che, T., Y. You, D. Wang, M. J. Tanner, V. M. Dixit, and X. Lin.** 2004. MALT1/paracaspase is a signaling component downstream of CARMA1 and mediates T cell receptor-induced NF-kappaB activation. J Biol Chem **279:**15870-6.

10. **Davis, M. M., J. J. Boniface, Z. Reich, D. Lyons, J. Hampl, B. Arden, and Y. Chien.** 1998. Ligand recognition by alpha beta T cell receptors. Annu Rev Immunol **16:**523-44.

11. **Deng, L., C. Wang, E. Spencer, L. Yang, A. Braun, J. You, C. Slaughter, C. Pickart, and Z. J. Chen.** 2000. Activation of the IkappaB kinase complex by TRAF6 requires a dimeric ubiquitin-conjugating enzyme complex and a unique polyubiquitin chain. Cell **103:**351-61.

12. **Dustin, M. L., S. K. Bromley, Z. Kan, D. A. Peterson, and E. R. Unanue.** 1997. Antigen receptor engagement delivers a stop signal to migrating T lymphocytes. Proc Natl Acad Sci U S A **94:**3909-13.

13. **Dustin, M. L., M. W. Olszowy, A. D. Holdorf, J. Li, S. Bromley, N. Desai, P. Widder, F. Rosenberger, P. A. van der Merwe, P. M. Allen, and A. S. Shaw.** 1998. A novel adaptor protein orchestrates receptor patterning and cytoskeletal polarity in T-cell contacts. Cell **94:**667-77.

14. **Egawa, T., B. Albrecht, B. Favier, M. J. Sunshine, K. Mirchandani, W. O'Brien, M. Thome, and D. R. Littman.** 2003. Requirement for CARMA1 in antigen receptor-induced NF-kappa B activation and lymphocyte proliferation. Curr Biol **13:**1252-8.

15. **Fanning, A. S., and J. M. Anderson.** 1999. Protein modules as organizers of membrane structure. Curr Opin Cell Biol **11:**432-9.

16. **Farinha, P., and R. D. Gascoyne.** 2005. Molecular pathogenesis of mucosa-associated lymphoid tissue lymphoma. J Clin Oncol **23:**6370-8.

17. **Ferraccioli, G. F., D. Sorrentino, S. De Vita, L. Casatta, A. Labombarda, C. Avellini, R. Dolcetti, D. Di Luca, C. A. Beltrami, M. Boiocchi, and E. Bartoli.** 1996. B cell clonality in gastric lymphoid tissues of patients with Sjogren's syndrome. Ann Rheum Dis **55:**311-6.

18. **Fischer, K. D., Y. Y. Kong, H. Nishina, K. Tedford, L. E. Marengere, I. Kozieradzki, T. Sasaki, M. Starr, G. Chan, S. Gardener, M. P. Nghiem, D. Bouchard, M. Barbacid, A. Bernstein, and J. M. Penninger.** 1998. Vav is a regulator of cytoskeletal reorganization mediated by the T-cell receptor. Curr Biol **8:**554-62.

19. **Gaide, O., B. Favier, D. F. Legler, D. Bonnet, B. Brissoni, S. Valitutti, C. Bron, J. Tschopp, and M. Thome.** 2002. CARMA1 is a critical lipid raft-associated regulator of TCR-induced NF-kappa B activation. Nat Immunol **3:**836-43.

20. **Gaide, O., F. Martinon, O. Micheau, D. Bonnet, M. Thome, and J. Tschopp.** 2001. Carma1, a CARD-containing binding partner of Bcl10, induces Bcl10 phosphorylation and NF-kappaB activation. FEBS Lett **496:**121-7.

21. **Germain, R. N.** 1997. T-cell signaling: the importance of receptor clustering. Curr Biol **7:**R640-4.

22. **Ghosh, S., M. J. May, and E. B. Kopp.** 1998. NF-kappa B and Rel proteins: evolutionarily conserved mediators of immune responses. Annu Rev Immunol **16:**225-60.

23. **Grakoui, A., S. K. Bromley, C. Sumen, M. M. Davis, A. S. Shaw, P. M. Allen, and M. L. Dustin.** 1999. The immunological synapse: a molecular machine controlling T cell activation. Science **285:**221-7.

24. **Harlow, E., D. Lane, and E. Harlow.** 1999. Using antibodies : a laboratory manual. Cold Spring Harbor Laboratory Press, Cold Spring Harbor, N.Y.

25. **Hofmann, R. M., and C. M. Pickart.** 1999. Noncanonical MMS2-encoded ubiquitin-conjugating enzyme functions in assembly of novel polyubiquitin chains for DNA repair. Cell **96:**645-53.

26. **Huang, J. F., Y. Yang, H. Sepulveda, W. Shi, I. Hwang, P. A. Peterson, M. R. Jackson, J. Sprent, and Z. Cai.** 1999. TCR-Mediated internalization of peptide-MHC complexes acquired by T cells. Science **286:**952-4.

27. **Hussell, T., P. G. Isaacson, J. E. Crabtree, and J. Spencer.** 1993. The response of cells from low-grade B-cell gastric lymphomas of mucosa-associated lymphoid tissue to Helicobacter pylori. Lancet **342:**571-4.

28. **Isaacson, P., and D. H. Wright.** 1983. Malignant lymphoma of mucosa-associated lymphoid tissue. A distinctive type of B-cell lymphoma. Cancer **52:**1410-6.

29. **Isaacson, P. G., and J. Spencer.** 1995. The biology of low grade MALT lymphoma. J Clin Pathol **48:**395-7.

30. **Isakov, N., and A. Altman.** 2002. Protein kinase C(theta) in T cell activation. Annu Rev Immunol **20:**761-94.

31. **Jain, J., C. Loh, and A. Rao.** 1995. Transcriptional regulation of the IL-2 gene. Curr Opin Immunol **7:**333-42.

32. **Jordan, M., A. Schallhorn, and F. M. Wurm.** 1996. Transfecting mammalian cells: optimization of critical parameters affecting calcium-phosphate precipitate formation. Nucleic Acids Res **24:**596-601.

33. **Jun, J. E., L. E. Wilson, C. G. Vinuesa, S. Lesage, M. Blery, L. A. Miosge, M. C. Cook, E. M. Kucharska, H. Hara, J. M. Penninger, H. Domashenz, N. A. Hong, R. J. Glynne, K. A. Nelms, and C. C. Goodnow.** 2003. Identifying the MAGUK protein Carma-1 as a central regulator of humoral immune responses and atopy by genome-wide mouse mutagenesis. Immunity **18:**751-62.

34. **Kane, L. P., J. Lin, and A. Weiss.** 2002. It's all Rel-ative: NF-kappaB and CD28 costimulation of T-cell activation. Trends Immunol **23:**413-20.

35. **Kappler, J. W., B. Skidmore, J. White, and P. Marrack.** 1981. Antigen-inducible, H-2-restricted, interleukin-2-producing T cell hybridomas. Lack of independent antigen and H-2 recognition. J Exp Med **153:**1198-214.

36. **Karin, M., and Y. Ben-Neriah.** 2000. Phosphorylation meets ubiquitination: the control of NF-[kappa]B activity. Annu Rev Immunol **18:**621-63.

37. **Kaye, J., S. Porcelli, J. Tite, B. Jones, and C. A. Janeway, Jr.** 1983. Both a monoclonal antibody and antisera specific for determinants unique to individual cloned helper T cell lines can substitute for antigen and antigen-presenting cells in the activation of T cells. J Exp Med **158:**836-56.

38. **Kolanus, W., W. Nagel, B. Schiller, L. Zeitlmann, S. Godar, H. Stockinger, and B. Seed.** 1996. Alpha L beta 2 integrin/LFA-1 binding to ICAM-1 induced by cytohesin-1, a cytoplasmic regulatory molecule. Cell **86:**233-42.

39. **Koseki, T., N. Inohara, S. Chen, R. Carrio, J. Merino, M. O. Hottiger, G. J. Nabel, and G. Nunez.** 1999. CIPER, a novel NF kappaB-activating protein containing a caspase recruitment domain with homology to Herpesvirus-2 protein E10. J Biol Chem **274:**9955-61.

40. **Lambert, C., N. Leonard, X. De Bolle, and E. Depiereux.** 2002. ESyPred3D: Prediction of proteins 3D structures. Bioinformatics **18:**1250-6.

41. **Lee, K. H., A. R. Dinner, C. Tu, G. Campi, S. Raychaudhuri, R. Varma, T. N. Sims, W. R. Burack, H. Wu, J. Wang, O. Kanagawa, M. Markiewicz, P. M. Allen, M. L. Dustin, A. K. Chakraborty, and A. S. Shaw.** 2003. The immunological synapse balances T cell receptor signaling and degradation. Science **302:**1218-22.

42. **Lee, K. H., A. D. Holdorf, M. L. Dustin, A. C. Chan, P. M. Allen, and A. S. Shaw.** 2002. T cell receptor signaling precedes immunological synapse formation. Science **295:**1539-42.

43. **Lee, K. Y., F. D'Acquisto, M. S. Hayden, J. H. Shim, and S. Ghosh.** 2005. PDK1 nucleates T cell receptor-induced signaling complex for NF-kappaB activation. Science **308:**114-8.

44. **Levine, E. G., D. C. Arthur, J. Machnicki, G. Frizzera, D. Hurd, B. Peterson, K. J. Gajl-Peczalska, and C. D. Bloomfield.** 1989. Four new recurring translocations in non-Hodgkin lymphoma. Blood **74:**1796-800.

45. **Li, Q., and I. M. Verma.** 2002. NF-kappaB regulation in the immune system. Nat Rev Immunol **2:**725-34.

46. **Lucas, P. C., M. Yonezumi, N. Inohara, L. M. McAllister-Lucas, M. E. Abazeed, F. F. Chen, S. Yamaoka, M. Seto, and G. Nunez.** 2001. Bcl10 and MALT1, independent targets of chromosomal translocation in malt lymphoma, cooperate in a novel NF-kappa B signaling pathway. J Biol Chem **276:**19012-9.

47. **McAllister-Lucas, L. M., N. Inohara, P. C. Lucas, J. Ruland, A. Benito, Q. Li, S. Chen, F. F. Chen, S. Yamaoka, I. M. Verma, T. W. Mak, and G. Nunez.** 2001. Bimp1, a MAGUK family member linking protein kinase C activation to Bcl10-mediated NF-kappaB induction. J Biol Chem **276:**30589-97.

48. **Meller, N., A. Altman, and N. Isakov.** 1998. New perspectives on PKCtheta, a member of the novel subfamily of protein kinase C. Stem Cells **16:**178-92.

49. **Monks, C. R., B. A. Freiberg, H. Kupfer, N. Sciaky, and A. Kupfer.** 1998. Three-dimensional segregation of supramolecular activation clusters in T cells. Nature **395:**82-6.

50. **Monks, C. R., H. Kupfer, I. Tamir, A. Barlow, and A. Kupfer.** 1997. Selective modulation of protein kinase C-theta during T-cell activation. Nature **385:**83-6.

51. **Nam, Y. J., K. Mani, A. W. Ashton, C. F. Peng, B. Krishnamurthy, Y. Hayakawa, P. Lee, S. J. Korsmeyer, and R. N. Kitsis.** 2004. Inhibition of both the extrinsic and intrinsic death pathways through nonhomotypic death-fold interactions. Mol Cell **15:**901-12.

52. **Nel, A. E.** 2002. T-cell activation through the antigen receptor. Part 1: signaling components, signaling pathways, and signal integration at the T-cell antigen receptor synapse. J Allergy Clin Immunol **109:**758-70.

53. **Newton, K., and V. M. Dixit.** 2003. Mice lacking the CARD of CARMA1 exhibit defective B lymphocyte development and impaired proliferation of their B and T lymphocytes. Curr Biol **13:**1247-51.

54. **Penninger, J. M., and G. R. Crabtree.** 1999. The actin cytoskeleton and lymphocyte activation. Cell **96:**9-12.

55. **Pomerantz, J. L., and D. Baltimore.** 2002. Two pathways to NF-kappaB. Mol Cell **10:**693-5.

56. **Pomerantz, J. L., E. M. Denny, and D. Baltimore.** 2002. CARD11 mediates factor-specific activation of NF-kappaB by the T cell receptor complex. Embo J **21:**5184-94.

57. **Rossman, J. S., N. G. Stoicheva, F. D. Langel, G. H. Patterson, J. Lippincott-Schwartz, and B. C. Schaefer.** 2006. POLKADOTS Are Foci of Functional

Interactions in T-Cell Receptor-mediated Signaling to NF-{kappa}B. Mol Biol Cell.

58. **Ruefli-Brasse, A. A., D. M. French, and V. M. Dixit.** 2003. Regulation of NF-kappaB-dependent lymphocyte activation and development by paracaspase. Science **302:**1581-4.

59. **Ruefli-Brasse, A. A., W. P. Lee, S. Hurst, and V. M. Dixit.** 2004. Rip2 participates in Bcl10 signaling and T-cell receptor-mediated NF-kappaB activation. J Biol Chem **279:**1570-4.

60. **Ruland, J., G. S. Duncan, A. Elia, I. del Barco Barrantes, L. Nguyen, S. Plyte, D. G. Millar, D. Bouchard, A. Wakeham, P. S. Ohashi, and T. W. Mak.** 2001. Bcl10 is a positive regulator of antigen receptor-induced activation of NF-kappaB and neural tube closure. Cell **104:**33-42.

61. **Ruland, J., G. S. Duncan, A. Wakeham, and T. W. Mak.** 2003. Differential requirement for Malt1 in T and B cell antigen receptor signaling. Immunity **19:**749-58.

62. **Ruland, J., and T. W. Mak.** 2003. From antigen to activation: specific signal transduction pathways linking antigen receptors to NF-kappaB. Semin Immunol **15:**177-83.

63. **Sachs, K., O. Perez, D. Pe'er, D. A. Lauffenburger, and G. P. Nolan.** 2005. Causal protein-signaling networks derived from multiparameter single-cell data. Science **308:**523-9.

64. **Saijo, K., I. Mecklenbrauker, A. Santana, M. Leitger, C. Schmedt, and A. Tarakhovsky.** 2002. Protein kinase C beta controls nuclear factor kappaB activation in B cells through selective regulation of the IkappaB kinase alpha. J Exp Med **195:**1647-52.

65. **Sampath, R., P. J. Gallagher, and F. M. Pavalko.** 1998. Cytoskeletal interactions with the leukocyte integrin beta2 cytoplasmic tail. Activation-dependent regulation of associations with talin and alpha-actinin. J Biol Chem **273:**33588-94.

66. **Schaefer, B. C., J. W. Kappler, A. Kupfer, and P. Marrack.** 2004. Complex and dynamic redistribution of NF-kappaB signaling intermediates in response to T cell receptor stimulation. Proc Natl Acad Sci U S A **101:**1004-9.

67. **Schaefer, B. C., T. C. Mitchell, J. W. Kappler, and P. Marrack.** 2001. A novel family of retroviral vectors for the rapid production of complex stable cell lines. Anal Biochem **297:**86-93.

68. **Schaefer, B. C., M. F. Ware, P. Marrack, G. R. Fanger, J. W. Kappler, G. L. Johnson, and C. R. Monks.** 1999. Live cell fluorescence imaging of T cell MEKK2: redistribution and activation in response to antigen stimulation of the T cell receptor. Immunity **11:**411-21.

69. **Scharschmidt, E., E. Wegener, V. Heissmeyer, A. Rao, and D. Krappmann.** 2004. Degradation of Bcl10 induced by T-cell activation negatively regulates NF-kappa B signaling. Mol Cell Biol **24:**3860-73.

70. **Schmitz, M. L., S. Bacher, and O. Dienz.** 2003. NF-kappaB activation pathways induced by T cell costimulation. Faseb J **17:**2187-93.

71. **Siegel, R. M., D. A. Martin, L. Zheng, S. Y. Ng, J. Bertin, J. Cohen, and M. J. Lenardo.** 1998. Death-effector filaments: novel cytoplasmic structures that recruit caspases and trigger apoptosis. J Cell Biol **141:**1243-53.

72. **Smith, K. A.** 1989. The interleukin 2 receptor. Annu Rev Cell Biol **5:**397-425.

73. **Srinivasula, S. M., M. Ahmad, J. H. Lin, J. L. Poyet, T. Fernandes-Alnemri, P. N. Tsichlis, and E. S. Alnemri.** 1999. CLAP, a novel caspase recruitment domain-containing protein in the tumor necrosis factor receptor pathway, regulates NF-kappaB activation and apoptosis. J Biol Chem **274:**17946-54.

74. **Stilo, R., D. Liguoro, B. Di Jeso, S. Formisano, E. Consiglio, A. Leonardi, and P. Vito.** 2004. Physical and functional interaction of CARMA1 and CARMA3 with Ikappa kinase gamma-NFkappaB essential modulator. J Biol Chem **279:**34323-31.

75. **Streubel, B., D. Huber, S. Wohrer, A. Chott, and M. Raderer.** 2004. Frequency of chromosomal aberrations involving MALT1 in mucosa-associated lymphoid tissue lymphoma in patients with Sjogren's syndrome. Clin Cancer Res **10:**476-80.

76. **Su, B., E. Jacinto, M. Hibi, T. Kallunki, M. Karin, and Y. Ben-Neriah.** 1994. JNK is involved in signal integration during costimulation of T lymphocytes. Cell **77:**727-36.

77. **Su, H., N. Bidere, L. Zheng, A. Cubre, K. Sakai, J. Dale, L. Salmena, R. Hakem, S. Straus, and M. Lenardo.** 2005. Requirement for caspase-8 in NF-kappaB activation by antigen receptor. Science **307:**1465-8.

78. **Su, T. T., B. Guo, Y. Kawakami, K. Sommer, K. Chae, L. A. Humphries, R. M. Kato, S. Kang, L. Patrone, R. Wall, M. Teitell, M. Leitges, T. Kawakami, and D. J. Rawlings.** 2002. PKC-beta controls I kappa B kinase lipid raft recruitment and activation in response to BCR signaling. Nat Immunol **3:**780-6.

79. **Sun, L., L. Deng, C. K. Ea, Z. P. Xia, and Z. J. Chen.** 2004. The TRAF6 ubiquitin ligase and TAK1 kinase mediate IKK activation by BCL10 and MALT1 in T lymphocytes. Mol Cell **14:**289-301.

80. **Sun, Z., C. W. Arendt, W. Ellmeier, E. M. Schaeffer, M. J. Sunshine, L. Gandhi, J. Annes, D. Petrzilka, A. Kupfer, P. L. Schwartzberg, and D. R. Littman.** 2000. PKC-theta is required for TCR-induced NF-kappaB activation in mature but not immature T lymphocytes. Nature **404:**402-7.

81. **Takeuchi, O., and S. Akira.** 2001. Toll-like receptors; their physiological role and signal transduction system. Int Immunopharmacol **1:**625-35.

82. **Thome, M., F. Martinon, K. Hofmann, V. Rubio, V. Steiner, P. Schneider, C. Mattmann, and J. Tschopp.** 1999. Equine herpesvirus-2 E10 gene product, but not its cellular homologue, activates NF-kappaB transcription factor and c-Jun N-terminal kinase. J Biol Chem **274:**9962-8.

83. **Tian, M. T., G. Gonzalez, B. Scheer, and A. L. DeFranco.** 2005. Bcl10 can promote survival of antigen-stimulated B lymphocytes. Blood **106:**2105-12.

84. **Uren, A. G., K. O'Rourke, L. A. Aravind, M. T. Pisabarro, S. Seshagiri, E. V. Koonin, and V. M. Dixit.** 2000. Identification of paracaspases and metacaspases: two ancient families of caspase-like proteins, one of which plays a key role in MALT lymphoma. Mol Cell **6:**961-7.

85. **Verweij, C. L., M. Geerts, and L. A. Aarden.** 1991. Activation of interleukin-2 gene transcription via the T-cell surface molecule CD28 is mediated through an NF-kB-like response element. J Biol Chem **266:**14179-82.

86. **Villalba, M., N. Coudronniere, M. Deckert, E. Teixeiro, P. Mas, and A. Altman.** 2000. A novel functional interaction between Vav and PKCtheta is required for TCR-induced T cell activation. Immunity **12:**151-60.

87. **von Haller, P. D., S. Donohoe, D. R. Goodlett, R. Aebersold, and J. D. Watts.** 2001. Mass spectrometric characterization of proteins extracted from Jurkat T cell detergent-resistant membrane domains. Proteomics **1:**1010-21.

88. **Wang, C., L. Deng, M. Hong, G. R. Akkaraju, J. Inoue, and Z. J. Chen.** 2001. TAK1 is a ubiquitin-dependent kinase of MKK and IKK. Nature **412:**346-51.

89. **Wang, D., Y. You, S. M. Case, L. M. McAllister-Lucas, L. Wang, P. S. DiStefano, G. Nunez, J. Bertin, and X. Lin.** 2002. A requirement for CARMA1 in TCR-induced NF-kappa B activation. Nat Immunol **3:**830-5.

90. **Weber, C. H., and C. Vincenz.** 2001. The death domain superfamily: a tale of two interfaces? Trends Biochem Sci **26:**475-81.

91. **Weiss, A., and D. R. Littman.** 1994. Signal transduction by lymphocyte antigen receptors. Cell **76:**263-74.

92. **Werlen, G., E. Jacinto, Y. Xia, and M. Karin.** 1998. Calcineurin preferentially synergizes with PKC-theta to activate JNK and IL-2 promoter in T lymphocytes. Embo J **17:**3101-11.

93. **Willis, T. G., D. M. Jadayel, M. Q. Du, H. Peng, A. R. Perry, M. Abdul-Rauf, H. Price, L. Karran, O. Majekodunmi, I. Wlodarska, L. Pan, T. Crook, R. Hamoudi, P. G. Isaacson, and M. J. Dyer.** 1999. Bcl10 is involved in t(1;14)(p22;q32) of MALT B cell lymphoma and mutated in multiple tumor types. Cell **96:**35-45.

94. **Woo, H. N., G. S. Hong, J. I. Jun, D. H. Cho, H. W. Choi, H. J. Lee, C. W. Chung, I. K. Kim, D. G. Jo, J. O. Pyo, J. Bertin, and Y. K. Jung.** 2004. Inhibition of Bcl10-mediated activation of NF-kappa B by BinCARD, a Bcl10-interacting CARD protein. FEBS Lett **578:**239-44.

95. **Yan, M., J. Lee, S. Schilbach, A. Goddard, and V. Dixit.** 1999. mE10, a novel caspase recruitment domain-containing proapoptotic molecule. J Biol Chem **274:**10287-92.

96. **Yeh, P. Y., S. H. Kuo, K. H. Yeh, S. E. Chuang, C. H. Hsu, W. C. Chang, H. I. Lin, M. Gao, and A. L. Cheng.** 2006. A pathway for tumor necrosis factor-alpha-induced Bcl10 nuclear translocation. Bcl10 is up-regulated by NF-kappaB and phosphorylated by Akt1 and then complexes with Bcl3 to enter the nucleus. J Biol Chem **281:**167-75.

97. **Zhang, Q., R. Siebert, M. Yan, B. Hinzmann, X. Cui, L. Xue, K. M. Rakestraw, C. W. Naeve, G. Beckmann, D. D. Weisenburger, W. G. Sanger, H. Nowotny, M. Vesely, E. Callet-Bauchu, G. Salles, V. M. Dixit, A. Rosenthal, B. Schlegelberger, and S. W. Morris.** 1999. Inactivating mutations and overexpression of BCL10, a caspase recruitment domain-containing gene, in MALT lymphoma with t(1;14)(p22;q32). Nat Genet **22:**63-8.

98.   **Zhou, H., M. Q. Du, and V. M. Dixit.** 2005. Constitutive NF-kappaB activation by the t(11;18)(q21;q21) product in MALT lymphoma is linked to deregulated ubiquitin ligase activity. Cancer Cell **7:**425-31.

99.   **Zhou, H., I. Wertz, K. O'Rourke, M. Ultsch, S. Seshagiri, M. Eby, W. Xiao, and V. M. Dixit.** 2004. Bcl10 activates the NF-kappaB pathway through ubiquitination of NEMO. Nature **427:**167-71.